Energy Conversion and Management: X 20 (2023) 100472

Contents lists available at ScienceDirect

Energy Conversion and Management: X

journal homepage: www.sciencedirect.com/journal/energy-conversion-and-management-x

Effects of step hole geometry and spray-wall interactions on spray atomization in LPDI injector

Young Soo Yu [a], Yubeen Yang [a], Seungho Yang [a], Dongheon Shin [a], Hoseung Yi [a], Namho Kim [a], Sungwook Park [b,*]

[a] Department of Mechanical Convergence Engineering, Graduate School of Hanyang University, 222 Wangsimni-ro, Seongdong-gu, Seoul 04763, Republic of Korea
[b] School of Mechanical Engineering, Hanyang University, 222 Wangsimni-ro, Seongdong-gu, Seoul 04763, Republic of Korea

ARTICLE INFO

Keywords:
Liquefied Petroleum Gas (LPG)
Spray-wall impingement
Phase Doppler Particle Analyzer (PDPA)
Nozzle hole geometry
LPG Direct Injection (LPDI)

ABSTRACT

The study aims to analyze the spray atomization of liquefied petroleum gas direct injection (LPDI) injector based on the macroscopic and microscopic experiments. Two experimental injectors were used in the presence and absence of step hole, and the experimental fuels used n-heptane and n-butane.

The macroscopic and microscopic spray characteristics as function of the application of step hole were analyzed using two experimental injectors and n-heptane fuel. The macroscopic spray experiments analyzed the initial spray, after the end of injection and nozzle tip wetting using near-field visualization, and microscopic spray experiment analyzed fuel–air atomization phenomenon as function of the application of step hole using PDPA equipment.

In addition, macroscopic and microscopic spray characteristics were analyzed for two experimental fuels and spray-wall impingement using the presence of step hole injector. The macroscopic spray experiment analyzed the spray evaporation characteristics for the two experimental fuels and spray-wall impingement using the schlieren visualization, and microscopic spray experiment analyzed the fuel–air atomization phenomenon as function of the two experimental fuels and spray-wall impingement using PDPA equipment.

It was found that the presence of step hole injector showed better atomization results than those of the absence of step hole injector. But, the tip wetting of the presence of step hole injector was poor than that of the absence of step hole injector. Furthermore, based on the schlieren experiment, a comparison of free and flat sprays with the two fuels found that the spray width and area of n-heptane in free spray exceeded those of n-butane owing to the vapor pressure of n-butane. However, in the flat spray, the spray width and area of n-butane were exceeded those of n-heptane. It was found that the atomization was promoted after the spray-wall impingement.

Introduction

Major countries around the world are gradually strengthening standards for vehicle emission regulations. The vehicle emission regulations of South Korea are differently applied for each vehicle fuel. Gasoline vehicle sold in South Korea are promoting the introduction of Low Emission Vehicle IV (LEV IV), which has been strengthened for new vehicles since 2026 based on U.S. emission regulations. The emission regulations of LEV IV include the reduction of hydrocarbon and nitrogen oxide emissions, and a more stringent the PM standard of the US06 mode from the current 4 mg/km to 2 mg/km by about 50 % [1]. In addition, diesel vehicles are promoting the introduction of Euro 7, which is more stringent for new light-duty vehicles after 2025 based on European emission (EU) regulations. For the first time after the introduction of EU regulations, gasoline and diesel vehicles were equally estimated from 2025, and strengthening the emission regulation of nitrogen oxides from 80 mg/km to 60 mg/km, and expanding the measurement range of particle number by more than 50 % from 23 nm to 10 nm. In addition, emission restrictions were established on previously unregulated pollutants (NH_3, brake were particles, etc) among air pollutants. The Euro 7 regulations strengthen all pollutants measured on the road and in the laboratory, and especially emissions measured on road strengthen emission pollutants of 55 % CO, 78 % NOx, and 69 % HC compared to the Euro 6 [2,3]. Among exhaust emissions from gasoline and diesel vehicles, the particulate matter and number have the disadvantage of adversely affecting environmental pollution such as fine dust, and harmful to the human body through the respiratory system [4,5].

* Corresponding author at: School of Mechanical Engineering, Hanyang University, 222 Wangsimni-ro, Seongdong-gu, Seoul 04763, Republic of Korea.
E-mail address: parks@hanyang.ac.kr (S. Park).

https://doi.org/10.1016/j.ecmx.2023.100472
Received 18 July 2023; Received in revised form 16 September 2023; Accepted 10 October 2023
Available online 13 October 2023

Nomenclature

D	**Droplet diameter**
P_{inj}	**Injection pressure**
P_{amb}	**Ambient pressure**
V	**Droplet velocity**
U_{inj}	**Injection velocity**
We	**Weber number**
ρ_{fuel}	**Fuel density**
σ	**Surface tension of fuel**

Abbreviations

AMD	**Arithmetic mean diameter**
BSFC	**Brake specific fuel consumption**
DI	**Direct injection**
ICE	**Internal combustion engine**
LDM	**Long distance microscope**
LPDI	**Liquefied petroleum gas direct injection**
LPG	**Liquefied petroleum gas**
PDPA	**Phase doppler particle analyzer**
PMT	**Photo multiplier tube**
SMD	**Sauter mean diameter**

Accordingly, many researchers in industries and academia around the world are conducting a lot of research in various fields to reduce the emissions and particle number from Internal Combustion Engine(ICE). For example, as a method to reduce the particle number in ICE, the efforts of increasing the fuel efficiency of ICE vehicles have been applied such as the development of high-performance engines [6–7] downsized engines [8], optimized combustion-chamber shape and fuel injection [9–10], reinforcement of cylinder flow [11], and use of alternative fuels [12–14]. Among alternative fuels, liquefied petroleum gas (LPG) is widely used. Because LPG fuels can be stored at low pressures, they offer the combined advantages of reduced air pollution, easy storage, low cost, sufficient fuel charging station infrastructure, lean combustion potential, and relatively simple hydrocarbons [15]. In addition, because the octane numbers of LPG components are similar to that of gasoline, it is possible to fuel a gasoline engine with LPG simply by modifying the fuel-injection system. Currently, gasoline and LPG engines use a direct injection (DI) method similar to diesel injection method. However, the spray structure and spray characteristics significantly change due to the difference in vapor pressure between LPG and gasoline fuel [15]. Y.S. Yu et al., investigated in detail the spray structure as function of fuel properties such as density, surface tension and vapor pressure using LPG fuels (propane, butane) and gasoline. They found that the flash boiling occurs due to differences in vapor pressure of test fuel and has a significant effect on spray characteristics. The difference in vapor pressure of the fuel causes flash boiling, which causes the spray structure, and this will be discussed in detail in section 3.2.

Furthermore, the replacement of PFI injector to DI injector to improve spray atomization have been applied. However, DI injector has the disadvantage of a short mixing formation time between spray and air [16–17]. To overcome this disadvantage, it is very important to improve the spray atomization in DI injector. Several factors can affect atomization of DI injectors, including high-pressure injection [18], flow within the injector nozzle [19], cavitation and flash boiling [20], and spray-wall impingement [21].

Here, the spray-wall impingement collision between the cylinder wall and the fuel is due to high-pressure injection and the narrow space of a downsized engine. Spray-wall impingement differs from free spray. In general, spray-wall impingement has high spatial dispersion and concentration of droplets and induces secondary breakup of injected fuel during collisions, allowing dispersion of fuel droplets in the entire space creating fine droplets. In addition, among various nozzle geometries of DI injector, the step hole has an important role on reducing deposit formation and increasing mixture formation of spray and air in cylinder owing to the reciprocal action for the spray and the nozzle wall inside the injector nozzle [22–24].

Lately, many research papers were published to investigate the influence for step hole on spray characteristics and the characteristics of spray-wall interaction, which has potent influence on fuel atomization, air pollutant levels and engine power.

R. Payri et al., [22,23] found that the counter-bore has the advantage of better fuel–air mixture for more air-entrainment. For this reason, it is the interaction between spray and recirculation air inside the counter-bore. In addition, they conducted the influence of the presence of counter-bore injector on combustion characteristics. There is an advantage that counter-bore nozzle has less Brake-specific fuel consumption (BSFC) and emits less CO and smoke than the standard nozzle. J. Park et al., [24] conducted the effects of different nozzle hole shapes on spray development. They reported that the smaller the diameter of step hole and the smaller the length of step hole, the stronger the vertical momentum. This is because reducing the diameter and length of step hole increases the air flow between wall and spray inside the step hole, reducing the radical direction and increasing the vertical momentum. H. Oh et al., [25] reported the results of spray, injector tip wetting and particulate emissions as function of various nozzle designs such as nozzle without step hole. They derived the correlation between spray and tip wetting depending on nozzle designs and suggested optimization method to reduce particulate emissions.

Pei et al., [26], who investigated the influence of impingement spray compared to free spray with various test fuels using phase Doppler anemometry. Furthermore, higher values of K, which is related to the Reynolds and Ohnesorge numbers, promoted finer breakup and smaller reflective droplets. Qiu et al., [27] compared free spray and spray impingement according to plate temperature under flash boiling conditions using various test methods. They found that the droplets of plate spray were slightly smaller than those of free spray at the same measurement point. Peraza et al., [28] described the macroscopic characteristics of spray-wall interaction as function of the wall inclination angle using optical equipment, such as schlieren and OH* chemiluminescence, which calculate the flame lift-off length, and natural luminosity diagnostics, which record how a flame spreads over a wall.

In this paper, the experimental study was conducted for the impacts of the application of step hole and the features of spray-wall interaction on spray atomization with LPG direct injection (LPDI) injector. Furthermore, the quantitative comparison of the effect of droplet phenomenon such as external flow break-up process and disturbance inside the step hole, on the initial spray shape from injector tip and average droplet characteristics. For the spray-wall impingement, the spray development process and spray atomization after spray-wall impingement were qualitatively and quantitatively analyzed owing to difference in vapor pressure with two fuels. Based on the two experiments, this paper provides data that can be used in future analysis of spray atomization.

Methodology

Experimental setup

Fig. 1(a) depicts that the nozzle internal shape and different hole layouts (with the presence and absence of step hole) of the three-hole injector. Both injectors have the same hole diameter. The presence of step hole injector has a L/D ratio of 1.1 and a step hole diameter of 0.35 mm while the absence of step hole injector has a L/D ratio of 1.5. Table 1 summarizes the fuel properties. One fuel is n-heptane, which has physical properties similar to those of gasoline [29]. In addition, LPG fuels are divided into winter and summer formulations. The fuel used in this study is the summer formulation, which n-butane is the main

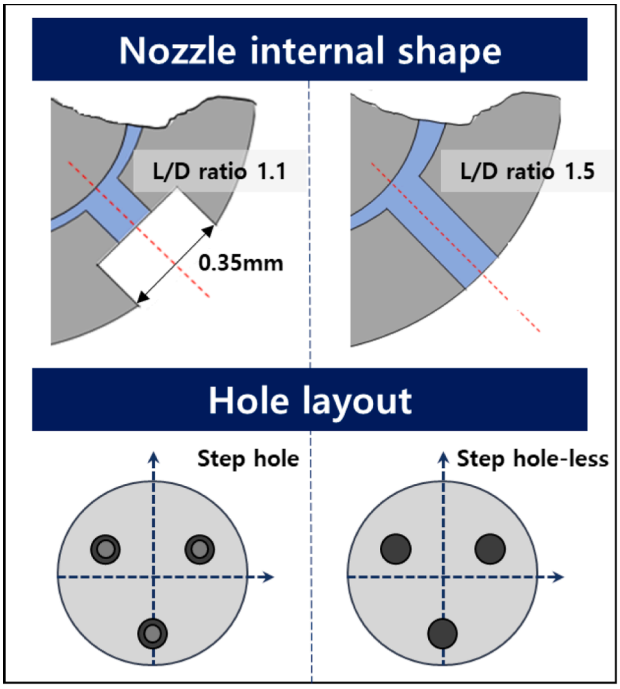

(a) schematic diagram of test injectors

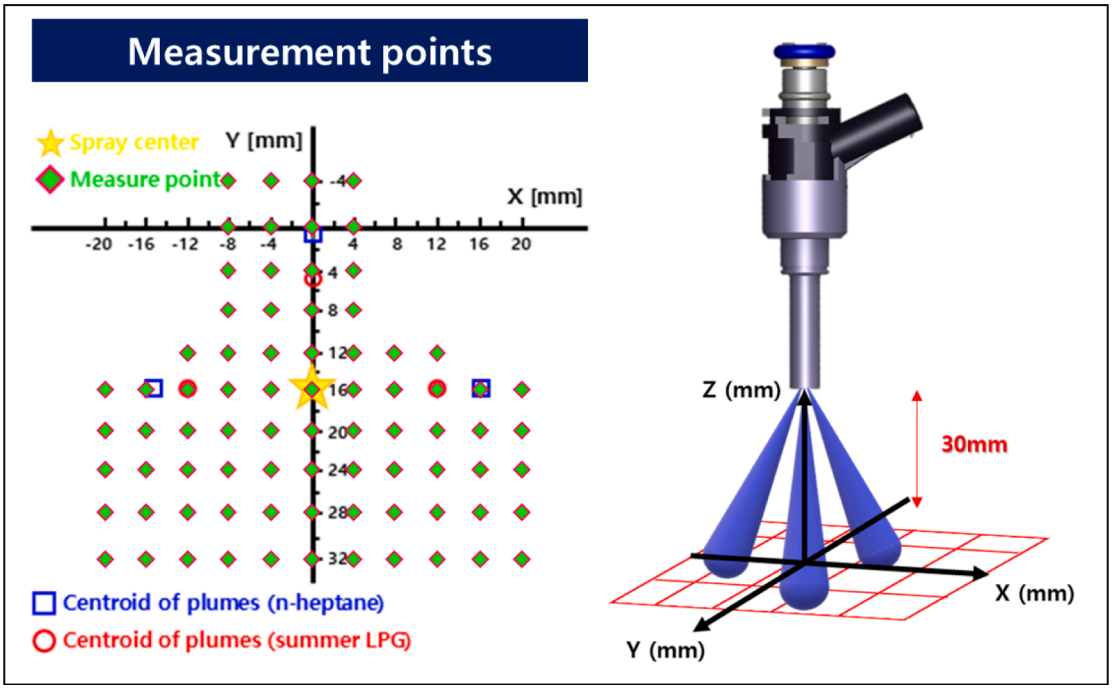

(b) measurement points as function of test fuels

Fig. 1. Experimental conditions.

component. LPG has the advantage of increased thermal efficiency and fewer harmful air pollutants than gasoline. Furthermore, the boiling point of LPG implies a lower transition temperature from liquid to vapor at atmospheric pressure compared with n-heptane, and the vapor pressure of LPG is relatively high, giving it excellent evaporation characteristics. This study analyzed the impacts of the two fuels on free spray and flat spray. To describe the impingement conditions with a piston inside the combustion chamber, this study involved manufacture of a flat acrylic model that included the impingement wall (Fig. 2).

The schematic diagram of the experiment is shown in Fig. 3 by dividing it into the application of step hole and the spray-wall impingement. The orientation and position of the camera and spray plumes of injector set in each experiment are shown in Fig. 3(c).

Fig. 3(a) is the schematic diagram of experiment for the application of step hole using n-heptane fuel. To visualize and investigate the spray atomization and droplet after injection, Fig. 3(a,i) and Fig. 3(a,iii) show the macroscopic spray experimental setup. In both experiments, high-power LED lamps (Cyclops I-120 W in Fig. 3(a.i), Veritas Constellation

Table 1
Properties of test fuels.

Fuel	n-heptane	n-butane
Chemical formula	C_7H_{16}	C_4H_{10}
Density (g/m^3@25℃)	0.68	0.57
Surface tension (mN/m@20℃)	20.14	0.023
Viscosity (cSt@20 ℃)	0.402	0.286
Vapor pressure (kPa)	4.6	213.7
Boiling point (℃)	98.5	−0.5

120E in Fig. 3(a,iii), ultra-high speed camera (Phantom, VEO1310), long-distance microscope (LDM, Model K2 DistaMaxTM) for near spray visualization were used. The near spray visualization images were obtained at a resolution of 640 × 144 and a recording rate of 90,000 fps, and the tip wetting visualization images were obtained at a resolution of 320 × 240 and a recording rate of 10,000 fps.

Fig. 3(b,iii) is the setup of the fuel supply system. To maintain high-pressure injection of a test injector, the fuel is pressurized to 150 bar using a pneumatic pump (Haskel, HSF-300). The test fuels were reserved in a fuel tank. The LPG was reserved in a 47 L gas cylinder. To create the liquid phase of n-butane, siphon method was used for the LPG fuel system. In detail, upper section inside the cylinder was pressurized using helium gas and the liquid was extracted from the bottom of the bombe using a long stainless steel tube.

Vapor-phase spray development was investigated using the schlieren method in shown Fig. 3(b,i). The primary notion of the schlieren method is to measure the change in index of refraction owing to fluid movement over the measuring area [30–31]. The detailed experimental setup was:

a) The light source was a high-intensity LED (Cyclops I-120 W) coupled with a pin-hole aperture placed on the emitter. The position of pin-hole was located at the focal point of a parabolic mirror.
b) To generate a collimated beam passing through the measurement area, one concave parabolic mirror was used.
c) The beam was converged by another concave parabolic mirror to focus the knife-edge just before the camera.
d) The position of the knife edge was adjusted to optimize the balance between schlieren sensitivity and intensity level.

Sequential spray images were obtained from a high-speed camera with a 200 mm macro lens (Nikon, Micro-NIKKOR) running at 10,000 fps (480 × 324 pixels).

Fig. 3(a,ii) and Fig. 3(b,ii) with geometric wall are a schematic of a Phase doppler particle analyzer (PDPA), detailed information for which is summarized in Table 2. The light source of a PDPA can measure the droplet diameter and velocity. The PDPA consisted of a 1.0 W argon-ion laser with a 514.5 nm Fiber light multi-color beam generator (2nd channel LDV.PDPA), laser source (Stellar-pro-L), 2D axis traverse, transmitter (TSI, TM250), receiver (TSI, RV2070), and Doppler signal analyzer (TSI, FSA4000, and PDM1000). Both the transmitter and receiver were mounted on a 2D axis traverse system to maintain a constant measurement angle to create a fringe pattern at the same point using two lasers. The ranges of droplet velocity and diameter of PDPA system were from –6.44 m/s to 109.42 m/s and 0 to 120 um, respectively. Multiple criteria, such as band pass filter, Photo multiplier tube (PMT) voltage, burst threshold, and signal-to-noise ratio, were applied to improve the accuracy and reliability of the measurements. For each point, the software analyzed a minimum of 5,000 valid droplets to ensure statistical significance and reproducibility. The arithmetic mean diameter (AMD) and Sauter mean diameter (SMD) were calculated from the measured droplet diameters:

$$\mathrm{AMD} = \frac{\sum n_i D_i}{\sum n_i}, \mathrm{SMD} = \frac{\sum n_i D_i^3}{\sum n_i D_i^2}$$

In Fig. 1(b), the droplet diameter and velocity were measured at 67 points with varying X and Y directions using the PDPA. The spray target coordinates of n-heptane and n-butane fuels are indicated by blue squares and red circles, respectively, and the spray center is indicated by a yellow star. Additionally, the measurement point was at a vertical length of 30 mm (z direction) based on injector tip. Comparing the spray target coordinates for the fuels, the n-butane fuel showed a narrower spray cross-sectional area and narrower spray plume coordinates compared with those of n-heptane due to its high evaporation property and relatively low density.

The detailed experimental conditions of step hole geometry and spray-wall interaction on spray atomization are listed in Table 3. The effect of step hole geometry on spray atomization was conducted for n-heptane. Furthermore, the effect of spray-wall interaction was conducted to compare the Weber number for spray-wall interaction using two experimental fuels (n-heptane and n-butane) and the presence of step hole injector.

2.2. Image post-processing sequence

The software program(MATLAB) was used to acquire quantitative macroscopic spray characteristics. The microscopic near spray measurement image was determined to calculate the spray characteristics, as shown in the left side of Fig. 4(a). After determining the microscopic near spray measurement image, post-processing occurred in the order of: raw image, adjust and gray image, binary image, and detected image. In the first adjust and gray step, RGB images 0 to 255 were switched into gray images 0 to 1 and the spray boundary was highlighted by darkening the around background. In the second binary step, the spray boundary was detected. Finally, the spray width and area were calculated by aggregating the pixels inside the spray boundary. Fig. 4(b) shows the image processing of droplets after spray in near spray visualization. The image post-processing sequence is the same as the one used for Fig. 4(a). Finally, in the tip wetting using LDM, ten images were obtained to

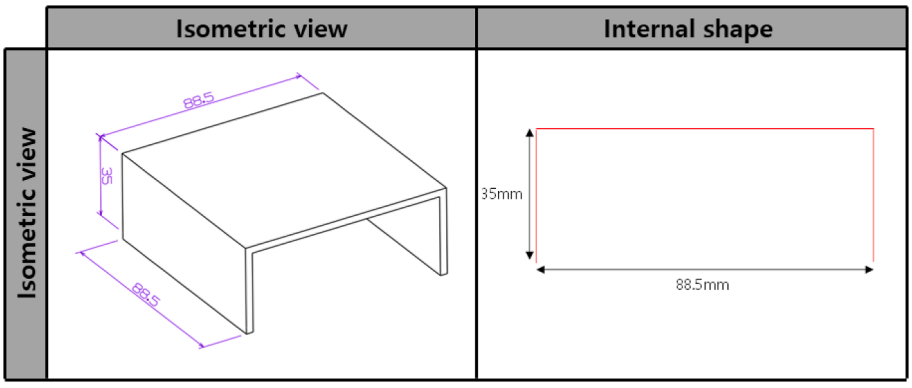

Fig. 2. Schematic diagram of the geometrical wall.

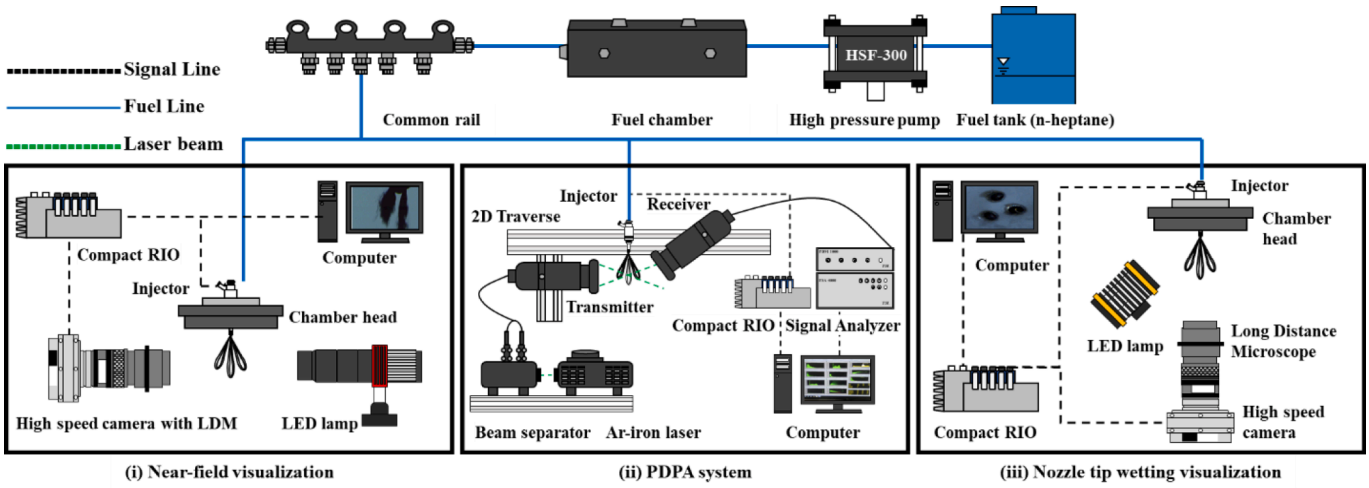

(a) The application of step hole experiment

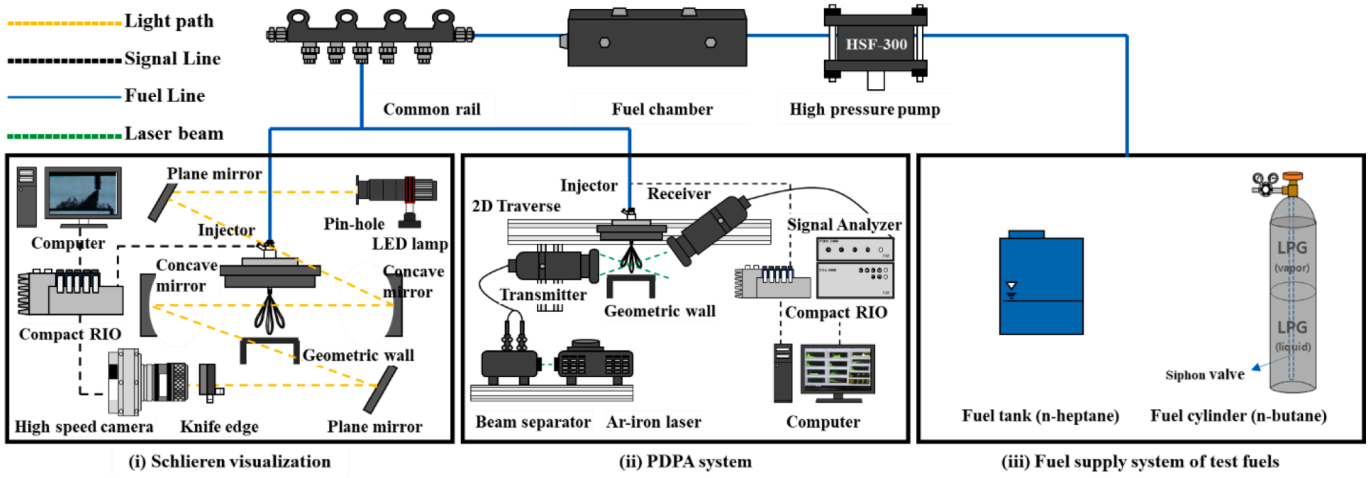

(b) Spray-wall impingement experiment

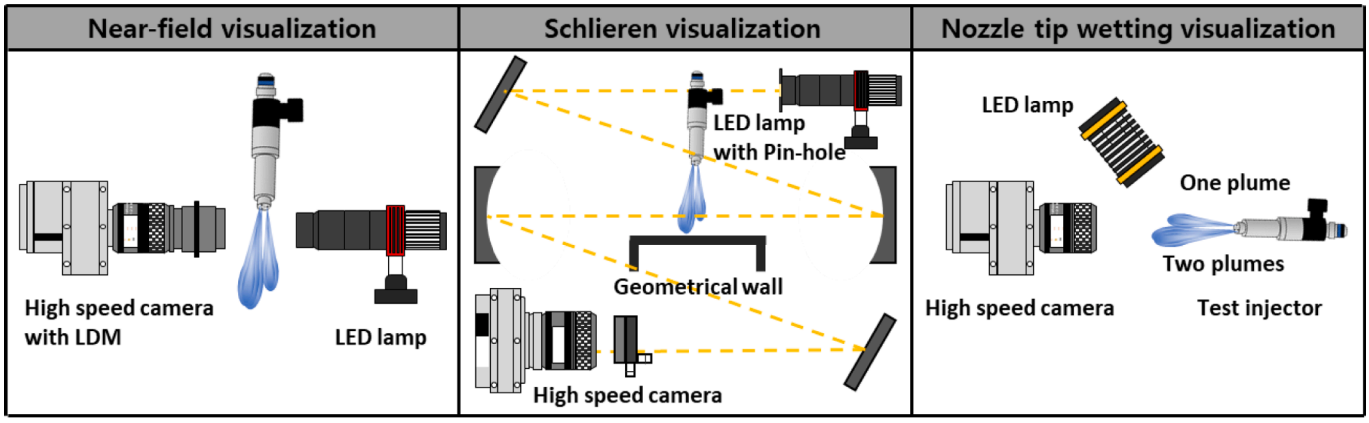

(c) Imaging orientation and position

Fig. 3. Schematic diagrams of experimental setup.

ensure reproducibility and reduce deviations between experiments in Fig. 4(c). To quantitatively analyze the tip wetting, the detailed test sequence can be found in the literature [15].

Fig. 4(d) is an image post-processing for schlieren image of the spray wall impingement. First, the raw image obtained by the high-speed camera is shown. The image was obtained by removing the background of a state in which fuel was not injected by the injector from all images collected after applying current to the injector. The color image

Table 2
Specifications of the PDPA system.

Droplet measurement system: PDPA	
Laser source	Argon-ion laser
Wavelength (mm)	514.5
Focal length (mm)	250 mm for transmitter optics 250 mm for receiver optics
Collection angle	33 (off-axis)
Beam diameter (mm)	1.77
Fringe spacing (mm)	6.4364

Table 3
Experimental conditions of the spray visualization and PDPA experiments.

	Spray visualization			PDPA
	Near-field	**Tip wetting**	**Schlieren**	
Ambient pressure (bar)	Atmospheric			
Ambient temperature (℃)	25			
Injection pressure (bar)	150			
Wall distance from the tip (mm)	–			30
Inj. energizing duration (ms)	1.5			

(24bit) was changed to a gray image (8bit), which was converted to a binary image to accelerate image processing and recognition calculations. A binary image can clearly select the spray boundary by converting a value above the threshold value from 0 to 1. The threshold value used in this study was 0.11. In addition, the definition of spray width is the distance to the edge of the spray boundary, meaning the horizontal length. The definition of spray area is the sum of all pixels within the spray boundary.

The spray that developed at the front was defined as forward, and the spray that developed to the rear was defined as backward according to the characteristics of development along the wall, as shown in Fig. 5(a). After spray impingement with an acrylic wall, the concept of spray path penetration (L_{path}) mentioned in Stanton et al., [32] was investigated to describe spray growth in Fig. 5(b). Here, the distance of the spray-wall impingement was L_x, and L_y was the point at which the spray was farthest sideways from the point of contact, with the wall vertically lowered based on the nozzle tip. The path penetration (dL_{path}) was first calculated with L_x and L_y. To illustrate the characteristics of spray development after spray wall impingement, the increase in the movement of spray path (dL_{path}) with respect to change in time can be calculated as follows:

$$dL_{path} = \sqrt{(dL_x)^2 + (dL_y)^2}$$

Spray path penetration (L_{path}) can be calculated by integrating the micro-change in the increased movement of the spray path (dL_{path}):

$$L_{path} = \int \sqrt{(\frac{dL_x}{dt})^2 + (\frac{dL_y}{dt})^2} dt$$

3. Experimental results and discussion

3.1. Impact of nozzle hole geometry on spray atomization

3.1.1. Spray visualization using LDM

Spray atomization is very important because it significantly affects thermal efficiency and engine power. To analyze the spray atomization qualitatively and quantitatively, many researchers have measured near-field images acquired from high-speed cameras equipped with microscopes [33–34]. However, unlike previous studies, in this paper, the impact of the presence and absence of step hole on atomization characteristics was analyzed by measuring the near-field images.

Fig. 6 depicts the sequential spray morphology of n-heptane in the near-field under the same injection pressure and atmospheric pressure conditions for two injectors. At 0.23 ms, two injectors started injection from the nozzle holes at the same point in time, and the spray morphology looked similar to each other. However, when the spray morphology was analyzed qualitatively, it was found that the spray width of the presence of step hole injector was larger than that of the absence of step hole injector. Fig. 7 quantitatively shows the spray width and spray area for ten test runs performed with each of two injectors at the same point in time. As a results, all experiments show that the presence of step hole injector has a larger spray width and spray area than that of the absence of the absence of step hole injector. Looking at this as a quantitative index, the average spray area of the presence of step hole injector was measured to be 23.9 % wider than that of the absence of step hole injector in Fig. 7(a), and the average spray width of the presence of step hole injector was measured to be about 10.3 % wider than that of the absence of step hole injector in Fig. 7(b). As illustrated in Fig. 8, this can be explained by two main causes. First, it is the impact of cavitation inside the nozzle hole. The two injectors are characterized by the presence or absence of step hole and different hole length. Here, the hole length is important parameter affecting the cavitation inside the nozzle hole. When fuel is injected from the sac volume to the nozzle hole, the cavitation inside the nozzle hole occurs due to the pressure difference. As in the absence of step hole injector in Fig. 8(a), as the hole length increases, the boundary layer of cavitation remains attached as the flow progresses. At this time, the discharge coefficient decreases due to the influence of the formed boundary layer, and the kinetic energy expanding in the radial expansion decreases [35]. In addition, when cavitation occurs more to the wall, the discharge coefficient decreases, the vertical momentum and turbulence intensity in the flow direction strengthened and the effect of atomization is enhanced, resulting in a decrease for radial momentum [36–37].

This is believed to be the cause of the small spray width and spray area in the absence of step hole injector. Additionally, as in the presence of step hole injector in Fig. 8(b), when the hole length is short, the radial velocity is relatively high owing to the impact of cavitation near the spray hole, resulting in increasing the spray angle. Second, the presence of step hole injector is atomized through active heat and mass transfer with the surrounding air. The second cause will be discussed in detail in section 3.2.

As shown in Fig. 6, as can be seen at 1.74 ms and 1.82 ms, the presence of step hole injector showed better atomization results than that of the absence of step hole injector. The droplet formed after spray was defined as the spray that had not fully developed following the completion of injection and was analyzed qualitatively and quantitatively. Fig. 9 shows the atomization characteristics after the end of injection. A perturbed fuel flow in the absence of step hole injector was observed. As you can show the red boxes, the absence of step hole injector formed larger droplets and ligaments than that of the presence of step hole injector. From the above-mentioned, the presence of step hole injector has an effect of atomization through heat and mass transfer with surrounding air. The larger droplets and ligaments can induce the formation of exhaust emissions(unburned hydrocarbons, PM and PN) [38]. Fig. 10(a) shows quantitatively the pixel number of droplet after spray from 1.76 ms to 2.11 ms. In all experiments, the absence of step hole injector, which has poor atomization characteristics, lost the initial high nozzle exit velocity in the process of closing the needle, and thus an abundance of poor atomized droplets were measured. These causes can be verified in other papers. For example, R. Payri et al., [23] describes from the 1D spray model that the presence of step hole injector has a higher air-entrainment than that of the absence of step hole injector, and then this effect would potentially lead to a reduction in soot emissions during engine operation. To analyze the atomization characteristics after the end of injection, the results of the injection rate for test injectors are shown in Fig. 10(b). The opening and closing times of needle for test injectors were similar.

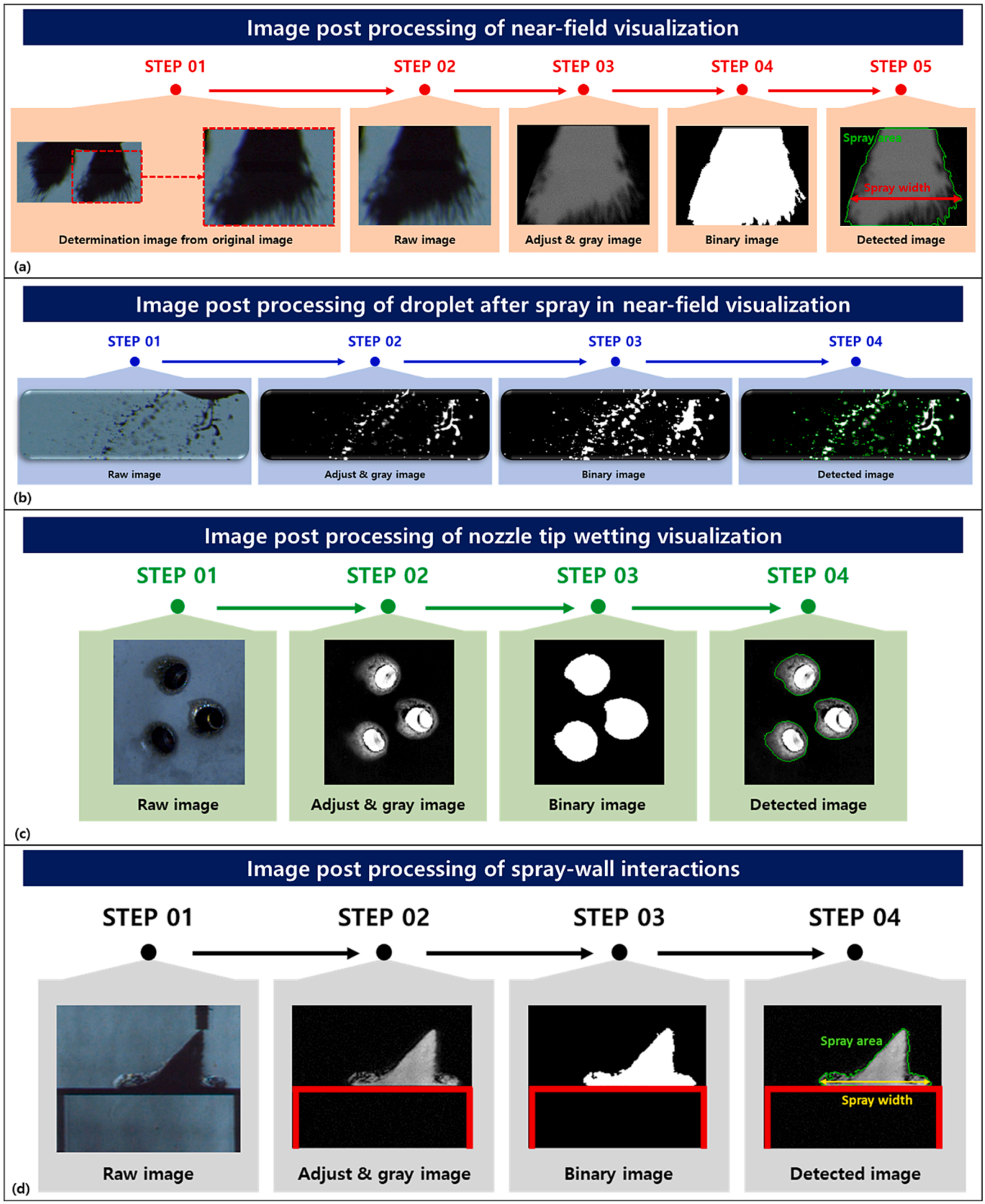

Fig. 4. Image post-processing of spray visualization.

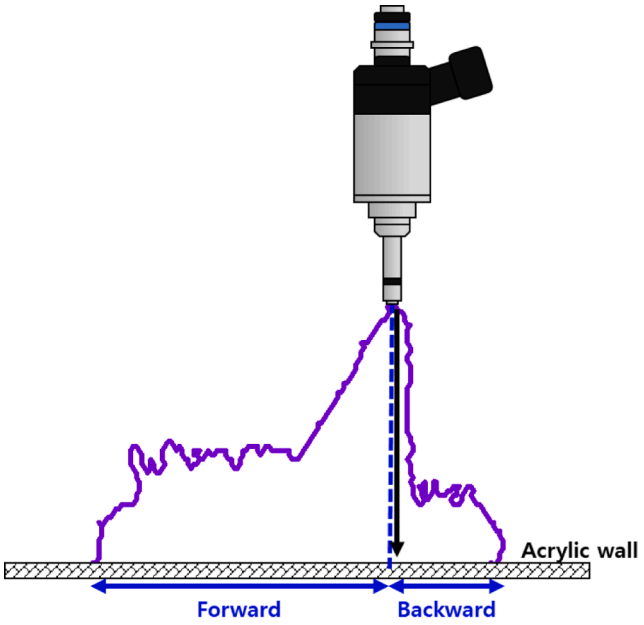

(a) Forward and backward of spray

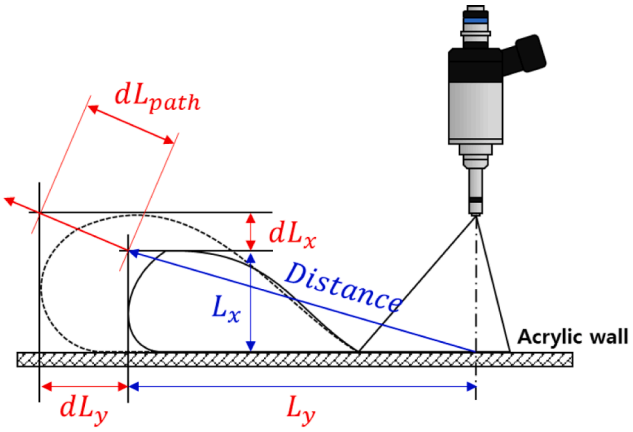

(b) spray path penetration

Fig. 5. Definitions of spray characteristics after spray wall impingement.

As a results in near-field visualization, consideration on the spray width and spray area of the two injectors is caused by the two causes from above-mentioned, but the primary breakup effect by cavitation is judged to be main effect on the initial spray width and spray area.

3.1.2. *Nozzle tip wetting in the near spray using LDM*

In this paper, nozzle tip wetting experiments were found by applying the application of cleaner and penetrant. Here, the cleaner was used to remove impurities on the injector surface, and the penetrant was used to evenly apply white color to the injector surface and photograph the area where the fuel was wet. The experimental procedure of the nozzle tip wetting experiments is detailed in a previous paper [15]. As can be seen from Fig. 11, it was qualitatively confirmed that the presence of step hole injector had a wider wet area than that of the absence of step hole injector. As mentioned earlier, it was believed that the spray width of the step hole injector was widened due to the spray liquid phase and air-entrainment of surrounding air; thus, the wet area was also expanded. Fig. 12(a) and (b) show quantitatively the wet area of the image measured through ten times. By comparing the results for the different injector nozzle hole geometries at 4.00 ms, the average wet area of the presence of step hole injector was measured to be 44.8 % higher than that of the absence of step hole injector. It is believed that the fuel absorbed by the penetrant does not evaporate, and the formed smaller droplets after the end of injection have a lower surface tension, resulting in a wider wet area. These causes will elucidate in more detail as follows. In this study, the wet area was identified by uniformly applying a cleaner

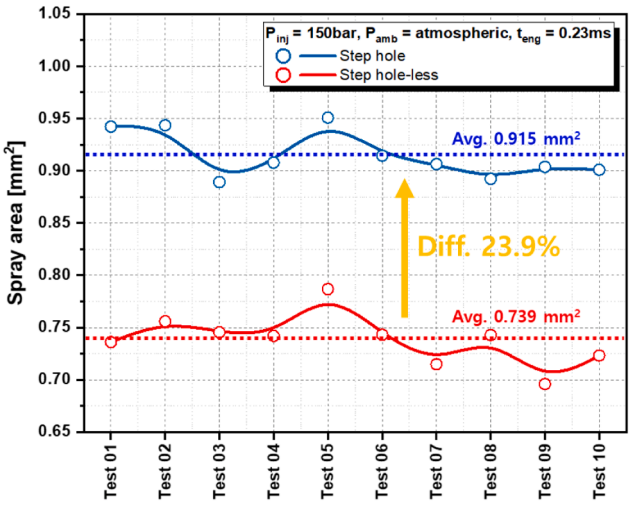

(a) Spray area

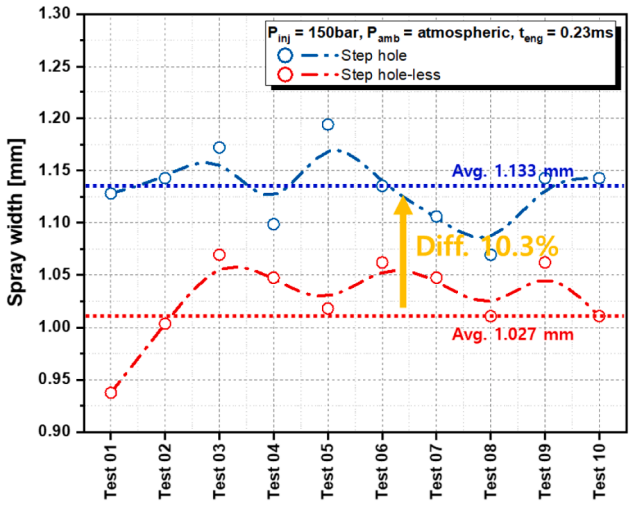

(b) Spray width

Fig. 7. Near-field spray characteristics as function of test injectors.

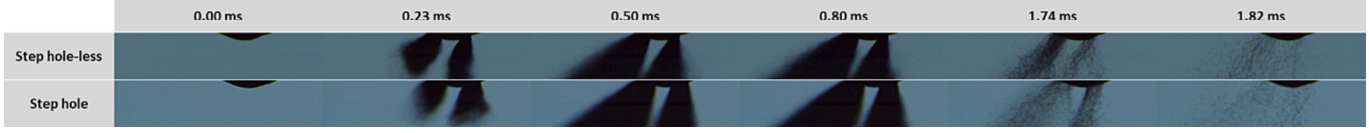

Fig. 6. Image sequence of the spray morphology in near-field visualization.

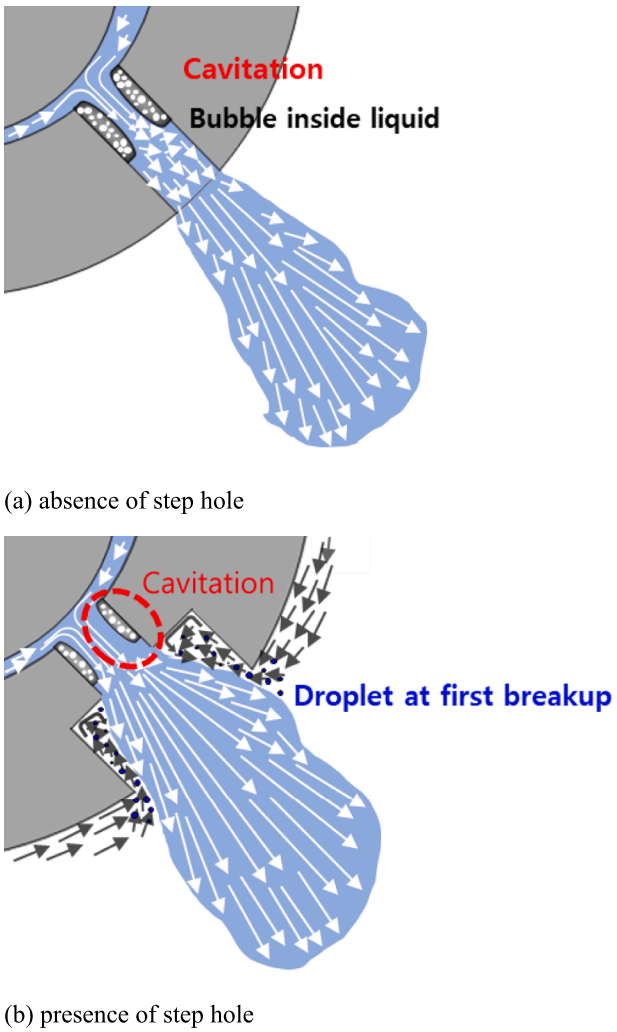

Fig. 8. Illustration of spray atomization as function of step hole geometry.

to the surface of the injector. At this time, the wet area is influencing the fuel properties. Here, the definition of surface tension is the force that contracts itself to reduce the surface area of the fuel, and if droplets are disrupted after the end of injection, the self-contracting force of the fuel weakens and then the surface tension gradually decreases, resulting in the spreading the fuel on the nozzle. Therefore, the wet area increases at 8.00 ms. In addition, the viscosity and vapor pressure of n-heptane fuel used in this study had no significant effect at room temperature. Therefore, the average wet area in the presence of step hole injector was measured to be 13.5 % higher than that of the absence of step hole injector. Fig. 13 compares the nozzle tip wetting boundary as function of the nozzle hole geometry at 4.00 ms and 8.00 ms. The blue line implies the wetting boundary in the presence of step hole injector and the black line implies the wetting boundary in the absence of step hole injector. The dotted area between the black and blue lines is the difference in the wet area of two injectors. The presence of step hole injector has a wider wet area than the absence of step hole injector. As previously mentioned, the absence of step hole injector using a large L/D ratio has a smaller spray width than that of the presence of step hole injector. If the spray width is small, the number of droplets colliding with the nozzle hole wall decreases, leading to reduction of the wet area. It can be qualitatively confirmed that the wet area was widened due to surface tension at 8.00 ms. This trend indicates that nozzle hole geometry affects spray characteristics such as spray structure at the initial time and atomization after end of injection and tip wetting phenomenon.

3.1.3. *Droplet atomization characteristics using PDPA system*

The techniques for measuring droplets injected from an injector nozzle are divided into mechanical drop-collecting techniques and optical techniques. The mechanical techniques are simple to use but have the disadvantage of interfering with the spray flow during the measurement process. The optical techniques have the advantage of not interfering with the spray flow, but they are expensive and require advanced operation skill [39]. Among the optical techniques, the PDPA system, which can concurrently quantify the droplet diameter and velocity, is commonly used through the fringe spacing, which is the intersection of two separated lasers [40–41]. The detailed principles of the PDPA system can be found in the literature [42]. In this paper, the droplet diameter and velocity were quantified to comprehend the effect of step hole geometry on atomization characteristics.

Fig. 14 depicts the comparison of spatial dispersion of droplet diameter and velocity as function of two injectors. It can be found through the contour bar of SMD that the droplet diameter increases as the color goes red, and the droplet diameter decreases as the color goes blue. In addition, owing to the impact of better air-entrainment inner section of the step hole and the interaction between spray plumes, the droplet diameter of the presence of step hole injector was overall smaller than that of the droplet size in the absence of step hole injector. The deliberation of theses causes will be elucidated in more detail as follows. The spray atomization consists of a primary breakup in which the liquid ligament and liquid film are disrupted and a secondary breakup in which the droplets formed continue to be disrupted into smaller droplets due to interaction with the surrounding air and air drag. The liquid ligament or liquid film spouted from the nozzle generates unstable waves in the step hole wall due to the ambient air, leading to an aerodynamic breakup in which a part of the liquid breaks away from droplets. In this case, unstable small disturbance generated in the liquid ligament and liquid film gradually grows with an aerodynamic force, which causes disruption to increase spray width. Therefore, the interplay between spray and the ambient air inside the presence of step hole was active than that of the absence of step hole and thereby, the spray width was wider due to disruption by aerodynamic force affected by the rough surface of the liquid ligament.

By comparing the spatial dispersion of droplet diameter of two

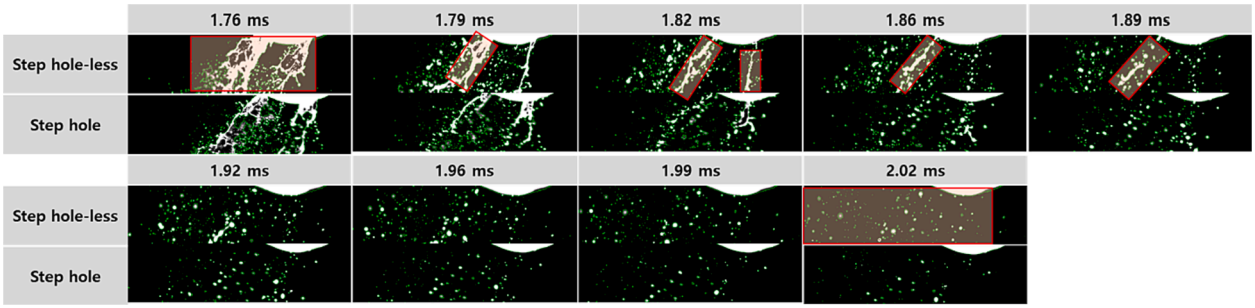

Fig. 9. Spray detected image sequence after energizing time in the near-field visualization.

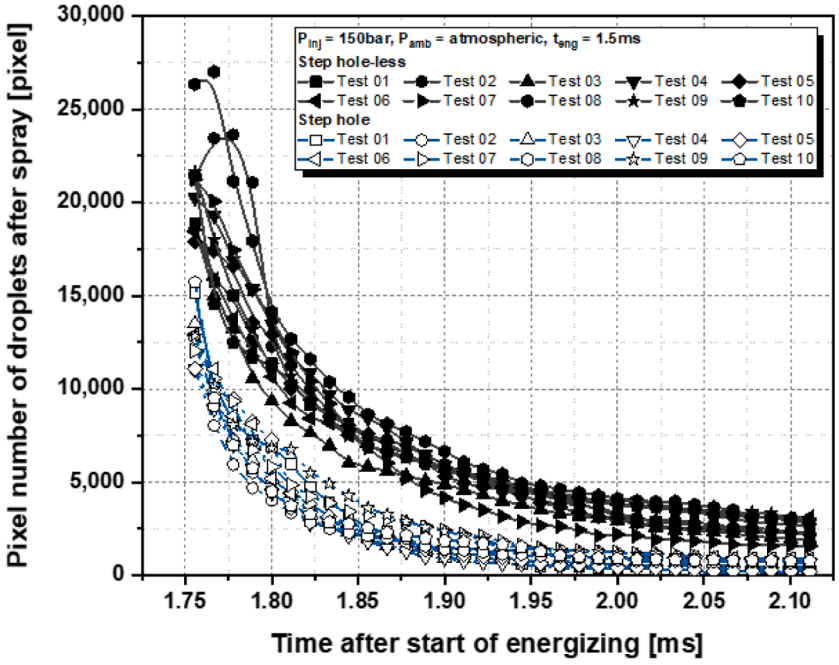

(a) Number of pixel after the end of injection

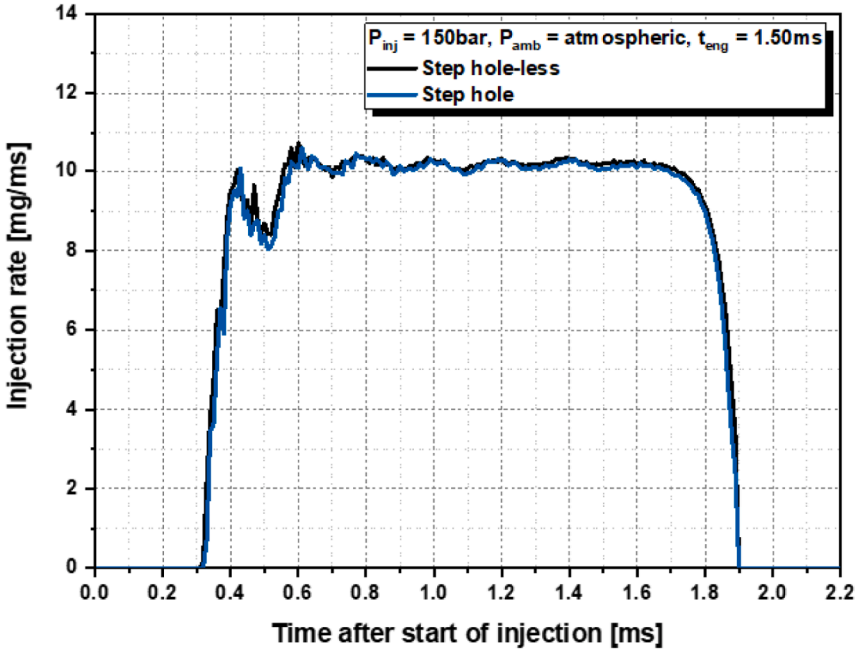

(b) Injection rate

Fig. 10. End of injection and injection rate characteristics as function of test injectors.

injectors, the absence of step hole injector had a high proportion of large droplets in red color in most areas as well as between spray plumes. In addition, from above-mentioned, the kinetic energy in the radial explosion decreased and the spray developed in the axial direction, resulting in large droplets due to without interaction between spray plumes. On the contrastively, in the presence of step hole injector, the droplet diameter becomes smaller and the spray width becomes larger owing to the interplay between the spray and ambient air inside the step hole. The expansion of spray width results in interference between spray plumes. This interference between spray plumes results in interaction and collisions, resulting in the uniform spray droplets. Due to this reason, the overall SMD of the presence of step hole injector was smaller than that of the absence of step hole injector in the spray center. As shown in contour images of droplet velocity, the presence of step hole injector is more widely distributed than that of the absence of step hole injector. These results directly prove that the presence of step hole

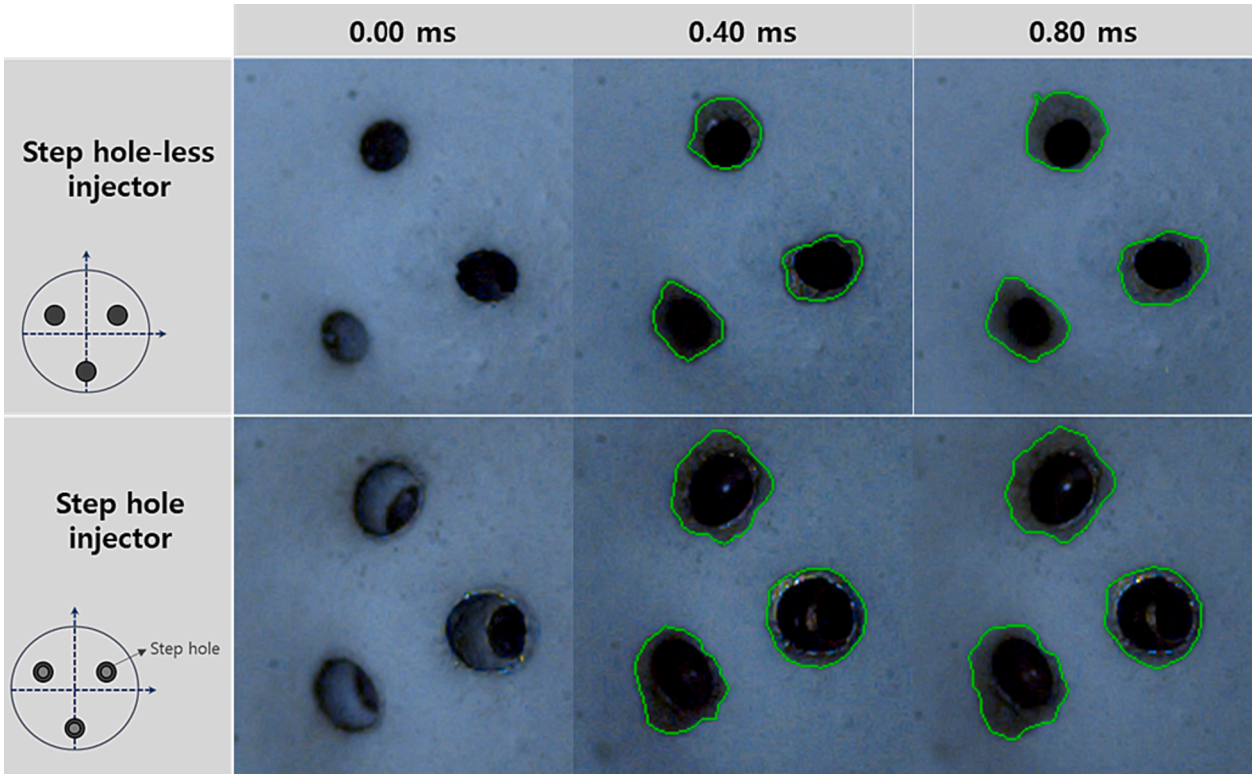

Fig. 11. Raw images with nozzle tip wetting boundary as function of hole geometry.

injector interacts more harmoniously with the surrounding air. It can be found that two injectors have a boundary area where the spray plumes interact with the surrounding air indicating several black arrows, where the velocity gradually slows down. In addition, the boundary area of each spray plume is clear in the absence of step hole injector, but the boundary area between spray plumes of the presence of step hole injector is not clear due to interplay between spray and surrounding air. These results suggest that the spray target may change owing to interplay between spray and ambient air, when the fuel temperature or ambient pressure increases.

Fig. 15(a) shows the comparison of droplet diameter and velocity at plume and spray center for two injectors. The red circle means the SMD, which is calculated at 0.3 ms intervals. The blue circle means the AMD and the gray circle means the entire droplet diameter during spray injection. The presence of step hole injector had a better atomization than that of the absence of step hole injector. Furthermore, at plume center, as shown red box, the droplet diameter of the presence of step hole injector was more measured than that of the absence of step hole injector in spray head. Since droplet diameters were improved owing to enhanced breakup and interaction between spray and around air. However, there was no significant difference between the averaged AMD and SMD on the spray head of two injectors. This is because the injector current is applied to the solenoid to supply continuous momentum to open the needle. After the spray head is passed, the droplets affected by the atomization were measured after the end of energizing duration on the spray tail. In these results, the droplet diameter of the absence of step hole injector was larger than that of the presence of step hole injector in the range from 25 to 45 um, resulting in the larger the AMD and SMD. These results were the same as those mentioned in section 3.1.1. In addition, more droplets of spray head were measured at plume center than that of spray center. In plume center, the spray droplets were continuously atomized and the droplet velocity was high. However, the atomized droplets in the three plumes were measured with low momentum. and then the velocity was low in the spray center. As illustrated in Fig. 15(b), it compares the droplet velocity at spray and plume center for two injectors. The droplet velocity of the presence of step hole injector was faster than that of the absence of step hole injector at spray and plume center. Because the spray width of the presence of step hole injector expanded due to droplet breakup, many droplets were separated, and then interaction occurred between droplets and around air.

Fig. 16 shows the statistical results of 5,000 valid data measured using PDPA experiment. The presence of step hole is shown in droplet distribution (a), cumulative droplet diameter (b), and droplet velocity distribution (c) for two injectors with presence or absence of step hole. Fig. 16(a) was similar to the above-mentioned result of Fig. 15(a). The AMD and SMD of two injectors were not significantly different, but the droplet diameters were measured slightly smaller in the presence of step hole injector. However, in the spray center, the presence of step hole injector was more measured in the range with a smaller droplet diameter than that of the absence of step hole injector. This is because the presence of step hole injector has excellent atomization performance in the spray tail, where the momentum supply was cut off and the atomization with the around air occurs. As shown in Fig. 16(b), the cumulative droplet diameter of two injectors is summarized. As mentioned above, there was no significant difference in the slope of the cumulative particle size of droplet using two injectors at the plume center, but the presence of step hole injector had a slightly larger slope due to its atomization performance. But, in the spray center, the presence of step hole injector was measured in a much smaller droplet diameter range than that of the absence of step hole injector, and the slope was large. In Fig. 16(c), the droplet velocity of the presence of step hole injector was slightly larger in the spray and plume center. As a results in PDPA experiment, consideration on the particle size of droplet of two injectors is caused by

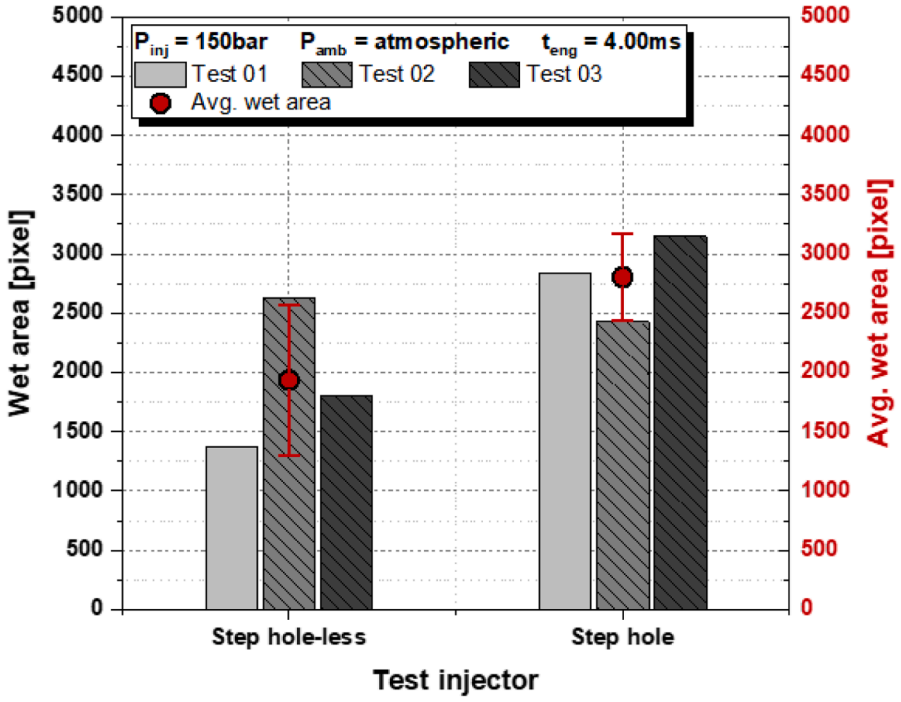

(a) T_{eng} = 4.00ms

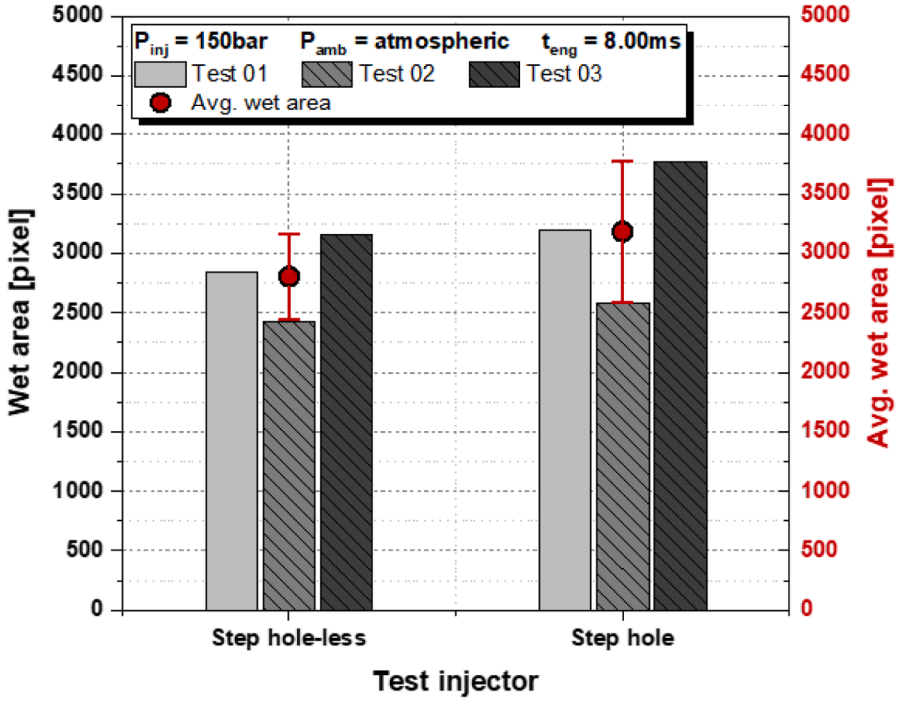

(b) T_{eng} = 8.00ms

Fig. 12. Comparisons of nozzle tip wetting as function of hole geometry.

the two causes from above-mentioned, but the secondary breakup effect by interaction between spray and around air is judged to be the main effect on the atomization of presence of the step hole. As a result of the section 3.1, the presence of step hole injector has a large wet area, which may have a coking problem due to combustion, but it is considered to be advantageous for combustion due to wits wide spray width and area and excellent spray atomization. Therefore, the experimental injector of spray-wall impingement applied in section 3.2 was studied with the presence of step hole injector.

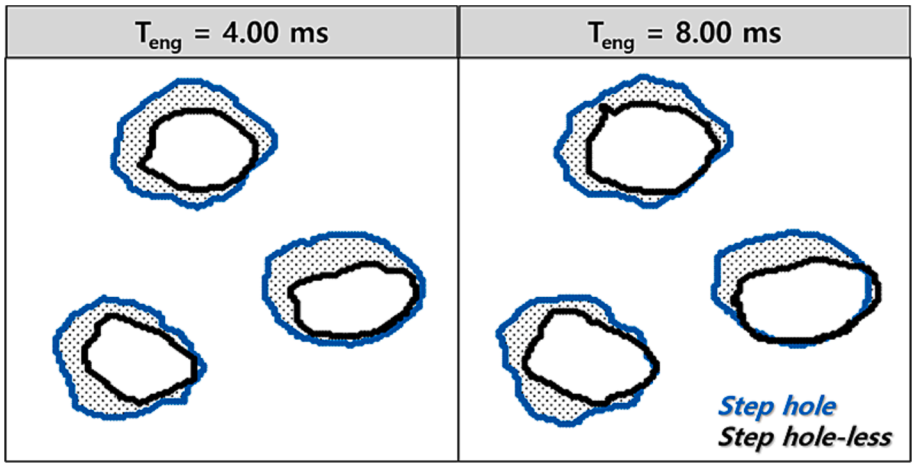

Fig. 13. Comparisons of nozzle tip wetting boundary as function of hole geometry.

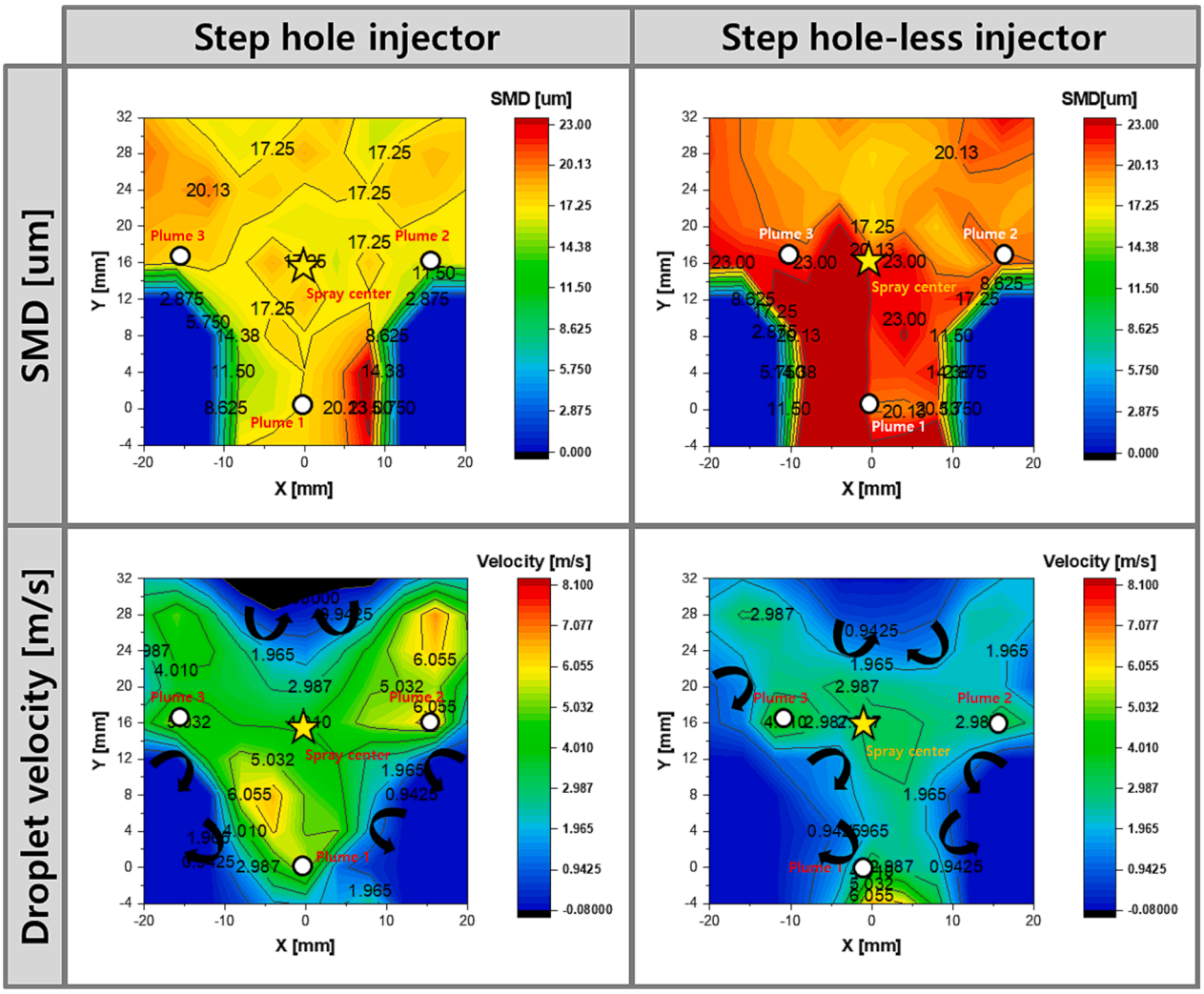

Fig. 14. Spatial dispersion of droplet diameter and velocity as function of two injectors.

3.2. Impact of spray-wall interactions on spray atomization

3.2.1. Spray vapor characteristics using schlieren method

Based on the schlieren experiment, Fig. 17 shows the evaporation characteristics of free and flat sprays using the two fuels. A comparison of free and flat sprays with the two fuels found that the spray width and area of n-heptane in free spray exceeded those of n-butane. This is because the vapor pressure of n-butane fuel is high — it vaporizes at ambient temperature and flash boiling occurs. At that point, the spray width and area narrow because the spray is agglomerated and well

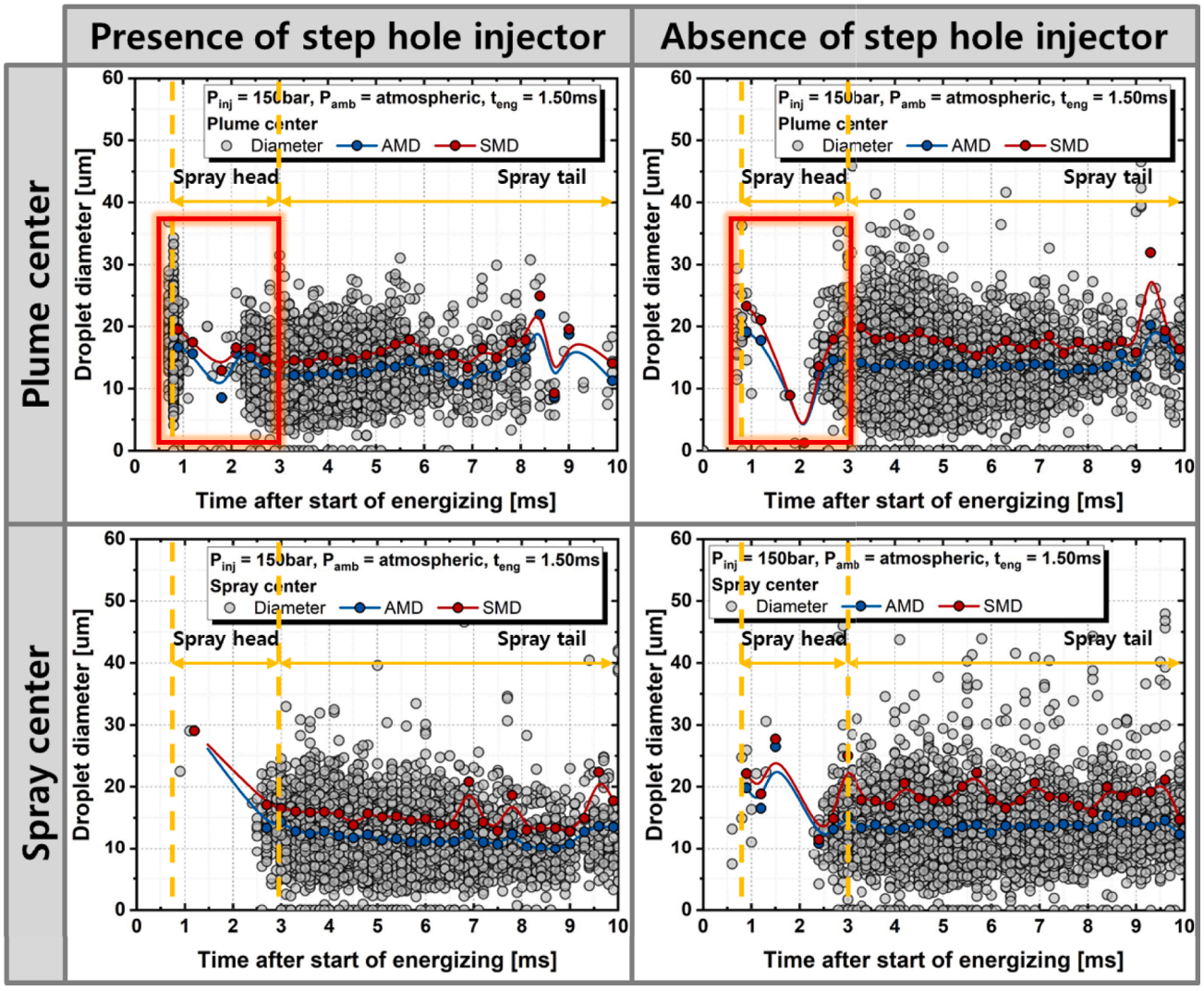

(a) Droplet diameter

Fig. 15. Comparison of SMD and droplet velocity at spray center as function of two injectors.

developed in the center. Here, generally, when flash boiling occurs, the spray width expands due to the expansion of volume as the phase changes from liquid to gas. However, in multi-hole injector, interactions between plumes cause them to come into contact with other plumes, resulting in spray collapse that merges into one, which enhances the drag force between relatively close plumes toward of the spray center. This is because adjacent spray plumes expanded by flash boiling are connected in a ring shape to form a closed area in the center of spray, preventing surrounding air from being transmitted from the outside to the closed center, which leads to a decrease in pressure. At this point, the spray develops into an agglomeration, reducing spray width and increasing penetration. For this reason, as shown in Fig. 17 in the red circle, n-heptane fuel is developed by clearly separating spray plumes as two and one sprays, whereas n-butane fuel is developed by combining three spray plumes.

However, in the flat spray, the spray width and area of n-butane fuel were exceeded those of n-heptane. This explains why, after the spray-wall impingement, atomization was promoted and the fuel evaporation characteristics of n-butane fuel was outstanding.

Fig. 18 depicts the quantitative spray width (a) and area (b). A comparison of the quantitative characteristics of free and flat sprays revealed that spray width increased and spray area decreased after wall impingement, likely owing to the diminishment of kinetic energy of the droplets after the flat spray, resulting in a decrease in spray area. Additionally, after the fuel was injected and collided with the wall, its axial momentum was converted into radial momentum, resulting in an increase in spray width. In free spray, the spray area increased because atomization was promoted by drag from the ambient air. When the spray width developed toward downward, the droplet velocity decreased because of the drag from the ambient air, reducing momentum severely.

Fig. 19(a) illustrates the spray boundary of two fuels at 1.5 ms after the start of energizing time. The forward and backward sprays of n-butane were longer than those of n-heptane because the spray-wall interaction increases not only the vapor pressure of the fuel, but also spray atomization. The width of forward spray for n-butane exceeded that of n-heptane, but the forward spray height for n-butane was smaller

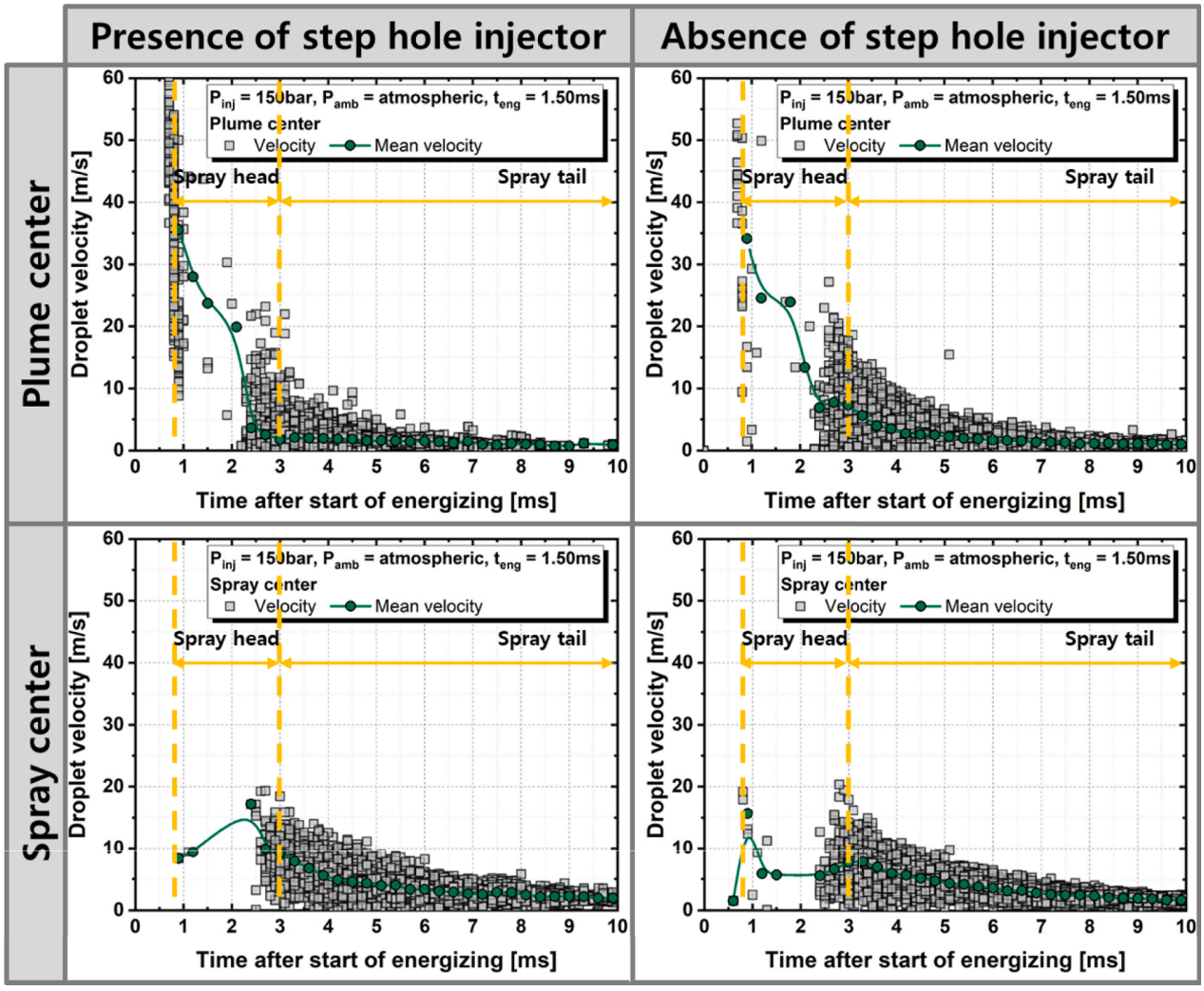

(b) Spray velocity

Fig. 15. (*continued*).

than that of n-heptane. In addition, the width and area of backward spray for n-butane exceeded those of n-heptane. The forward and backward spray characteristics of n-butane are critical when determining the mixture formation inside a combustion chamber. The height of forward spray for n-butane was lower in comparison with n-heptane, but the spray width was wide and the surface in contact with the surrounding air widened, encouraging fuel atomization. Also, the height and width in backward spray for n-butane were larger than those of n-heptane. Fig. 19(b) quantitatively presents the forward and backward spray characteristics. For both fuels, the forward and backward spray significantly increased after an injection time of 0.5 ms, at which point the spray collided with the wall. Although kinetic energy was lost due to the spray-wall interaction, because the droplet velocity of n-butane is fast and the initial velocity and momentum of the spray are large. The difference in droplet velocity between n-butane and n-heptane is discussed in section 3.2.2. Fig. 20(a) presents the spray boundary of the test fuels over time. Test fuels have an expanding spray boundary over time. n-Butane has the advantage of excellent forward and backward spray development and a large of backward. Unlike n-butane, and although the forward and backward sprays of n-heptane develop slowly, the height of the forward spray has the advantage of being large. The difference in spray characteristics for each fuel may exert a strong influence on mixture formation. Fig. 20(b) provides the quantitative data for the path penetration (L_{path}), which is characteristic of spray development after wall impingement. After an injection time of 0.5 ms, when the spray collided with the wall, n-butane had a higher evaporation property and droplet velocity compared to n-heptane, giving it the advantage of superior spray development due to improved evaporation.

3.2.2. *Droplet atomization characteristics using PDPA system*

Fig. 21 shows the spray atomization characteristics of free and flat sprays using the two fuels in the PDPA experiment. The three white stars indicate the spray plumes of the LPDI with three holes. A comparison of the droplet diameters of free and flat sprays showed that the atomization of free spray was superior to that of flat spray. As shown in Fig. 22, this is because of a vortex swirling in the opposite direction of the spray owing to air entrainment influenced by the interaction of the high-speed injection and the ambient air. The spray atomization performance improved, likely due to the effect of the vortex, which exerts a drag on the surrounding air. However, as indicated by the white dotted boxes, the SMD was large around the spray plume after spray-wall impingement. After the spray collided with the wall, it divided into small droplets that do not evaporate immediately but burst the cylinder wall or the piston and linear to form a wall film. When the wall film generated the cylinder wall or the surface of the wall collided with the high-speed fuel injected by the injector, some of the droplets split and splashed out

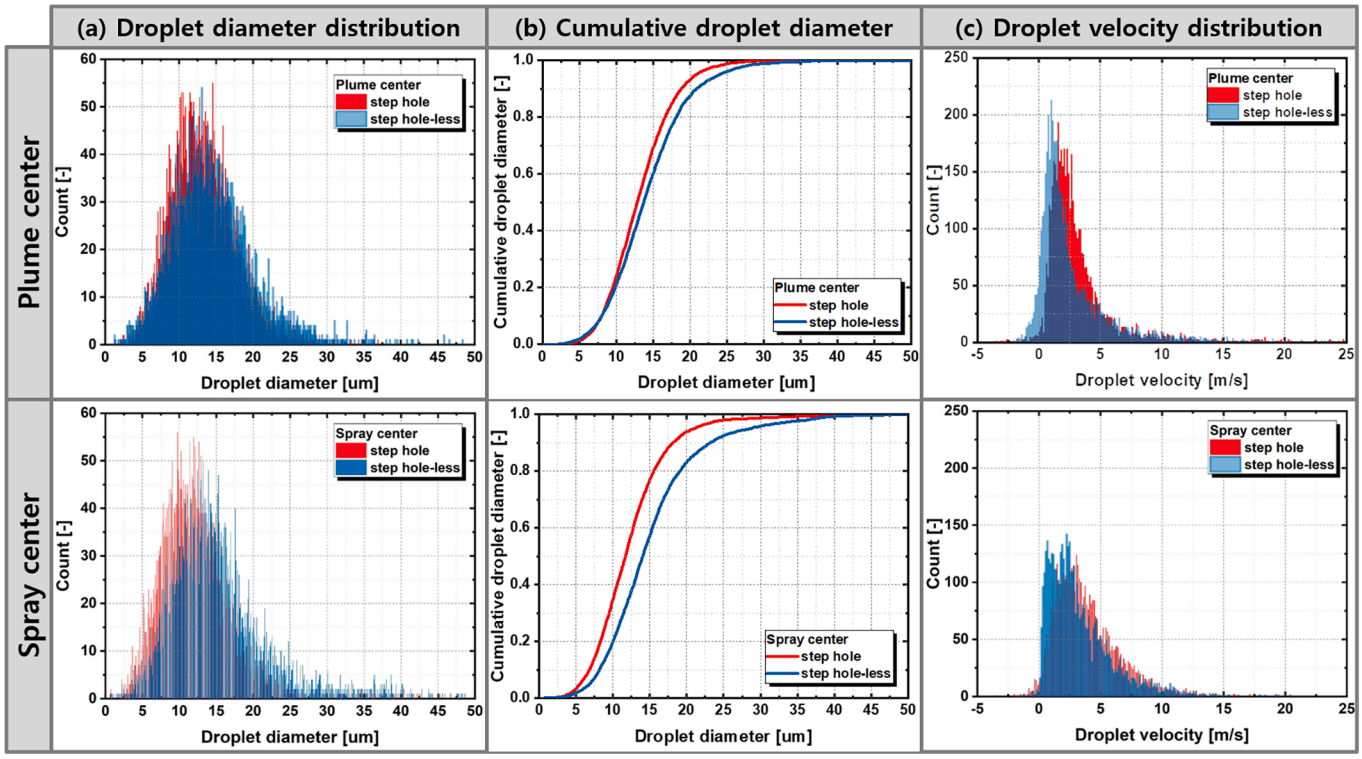

Fig. 16. Statistics characteristics at spray center as function of two injectors.

to form another fuel film. For this reason, both fuels are believed to have a large SMD around the spray plumes. This study compares spray atomization between test fuels. n-Butane exhibited superior spray atomization compared with n-heptane. This tendency likely improved spray atomization rapidly because of the high evaporation property of n-butane, which has excellent evaporation properties, low density, and surface tension.

Fig. 23 depicts the droplet velocity of the two fuels at various measurement points. The scale color bar confirms that the difference in droplet velocity between the two fuels was large. The difference is likely is due to fuel density at the same injection pressure and atmospheric pressure, as shown in equation.

$$U_{inj} = \sqrt{\frac{2(P_{inj} - P_{amb})}{\rho_{fuel}}}$$

The relatively high speed of n-butane is strongly affected by the air resistance of the ambient air, which also affects spray atomization. The air resistance of the ambient air causes turbulence and destabilizes the spray, leading to variations in droplet diameter and velocity. Both fuels are characterized by high droplet velocities around the spray plume but low droplet velocities in the middle and outside of the spray plume. However, if the droplet velocity is high, the coalescence effect between droplets is large and the rebound in the fuel film has the disadvantage of increasing the droplet diameter in the radial direction (i.e., along the × dimension). In addition, fuel injected at high speed is subjected to a wall-wetting phenomenon that is attached to the inner wall of the combustion chamber because of a large spray penetration. Comparing droplet velocity dispersion, n-butane was wider compared to n-heptane owing to the superior vapor pressure of n-butane. Additionally, the droplet velocity dispersion of free spray was broader in comparison with flat spray. It is because the spray area was widened by air entrainment (Fig. 22). A high droplet velocity favors the formation of a mixture due to superior spray atomization, but it is disadvantageous in terms of the coalescence effect between droplets and the wall wetting affected by the spray penetration. Additional research is needed to explore these competing issues. Suggested strategies include optimizing the spray target direction of the injector, adjusting injection parameters, and the use of renewable fuels (so-called electric fuels, or e-fuels).

Fig. 24 shows droplet diameters and velocities for the two fuels corresponding to plume 3 in free and flat sprays. The SMD of the free spray was measured more often than the SMD of the flat spray in the spray head and tail parts. After the spray-wall impingement, relatively few droplets were measured due to the secondary breakup of droplets in spray-wall impingement. In addition, n-butane fuels were measured less frequently because the fuel injected at high speeds quickly passed the probe through the laser intersection. Over time, the droplet diameter sizes of the two fuels were slightly different in free and flat sprays. n-Butane had a larger deviation of droplet diameter size in flat spray compared with free spray but has the advantage of improving spray atomization due to secondary breakup of droplets. However, because n-heptane has a lower vapor pressure and higher density than that of n-butane fuels, the droplet diameter was increased slightly due to the formation of a fuel film or rebound droplets.

In the spray head part (0.6 to 2.2 ms), n-heptane indicates a faster droplet velocity than that of n-butane in the initial section (0.5 to 1.2 ms). This may be due to the large SMD of n-heptane in the initial section, which is the section before active spray atomization. However, at 1.2 ms, the droplet velocity of n-butane is greater than that of n-heptane. Also, the droplet velocity dispersion of free spray was wider than that of flat spray for both fuels. For this reason, the spray momentum was lost and the droplet velocity was reduced due to friction with the surrounding air after the spray-wall impingement. The total amount of droplets in flat spray was greatly lower than that of free spray. A Doppler signal likely interfered with the effect of the droplets floating in the measurement region (or “fringe pattern”), where the lasers intersect. This could result in inaccuracies or inconsistencies in the measurement of droplet diameter and velocity, with a larger impact for flat spray.

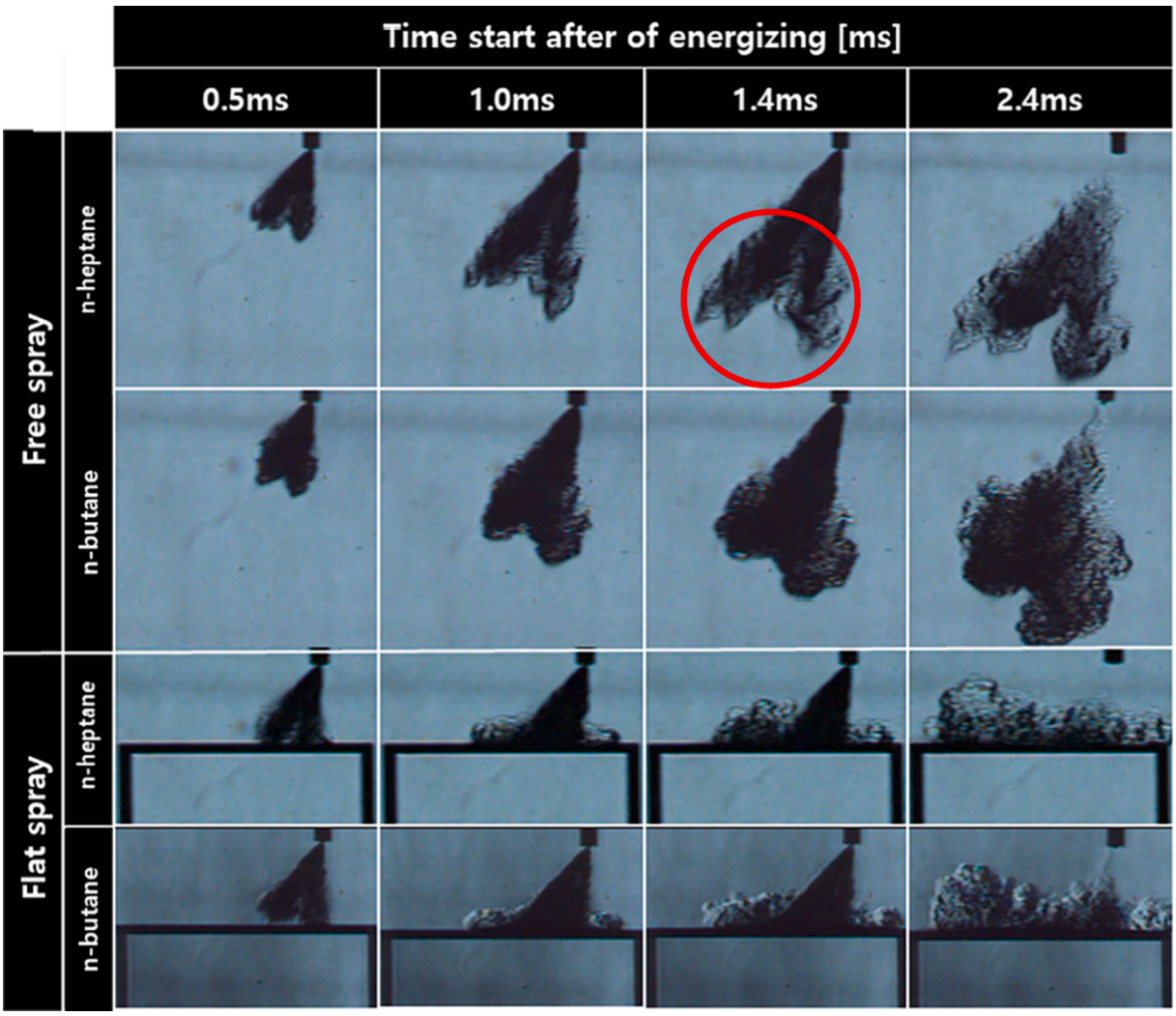

Fig. 17. Comparison of spray development between free spray and flat spray.

3.2.3. *Weber number characteristics*

The impingement process can express the relative force exerted on spray particles as Weber number and Reynolds number, which are functions of spray particle collision energy [43]. These parameters are used to quantify the relative force exerted during the impingement process. The effect on spray-wall impingement was analyzed using the Weber number. W. Qi et al [44] conducted a study on nozzle internal turbulence and disruption model using a spray/wall interaction model. Previous researchers have been conducting a variety of experimental and numerical studies on the spray/wall interaction model [45,46]. Fig. 25 shows the Weber numbers calculated using the droplet diameter and the velocity obtained by PDPA and fuel properties using equation (2).

$$\mathrm{We} = \frac{\rho_{fuel} v^2 D}{\sigma} \tag{2}$$

Here, the Weber number means as an index of the degree of kinetic energy relative to the surface tension of droplets. As a result of the experiment, the Weber number of n-butane was approximately 16 times larger than that of n-heptane, and the velocity of both fuels was greatest at the spray plume and nearby. In Fig. 26, which describes the condition after the spray collided with wall, the spray droplets can be classified into three categories: stick, spread, and splash, according to Weber number. As the Weber number increases from stick to splash, droplet collision energy increases and spray atomization is promoted. n-Butane exhibited superior atomization performance compared with that of n-heptane in free spray, but both fuels' Weber number increased in flat spray. Therefore, in terms of flat spray, it can be assumed that the fuel collided with the fuel film created spread at high speed, and the droplets were disrupted and bounced in the radial explosion, leading to a large SMD around the spray plume.

4. Conclusion

The experimental study was conducted for the application of step hole and the characteristics of spray-wall interaction on spray atomization with LPDI injector. The spray development process and atomization for the impact of step hole geometry and spray-wall interaction were qualitatively and quantitatively analyzed. The major results of this study are drawn as follows:

Based on the near-field experiments, the presence of step hole injector was measured to have an average spray area 23.9 % larger than that of the absence of step hole injector. Additionally, the average spray width was 10.3 % wider than that of the absence of step hole injector. Furthermore, the presence of step hole injector showed better atomization results than those of the absence of step hole injector at the end of injection.

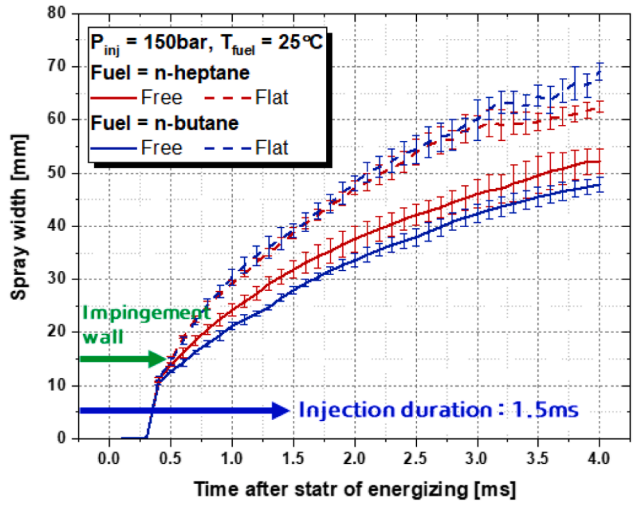

(a) Spray width

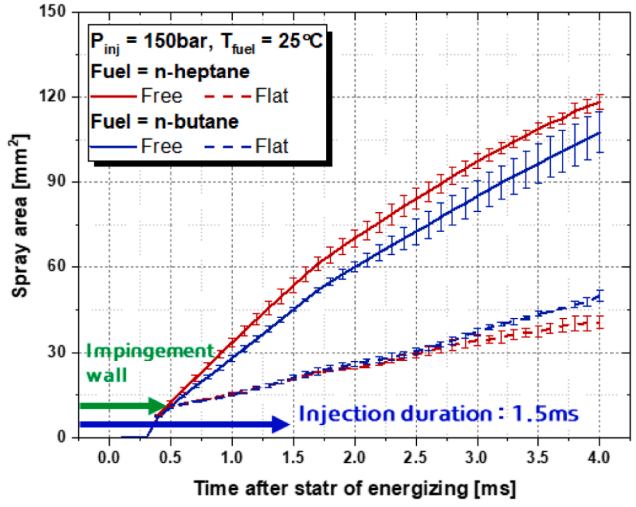

(b) Spray area

Fig. 18. Macroscopic spray characteristics between free spray and flat spray.

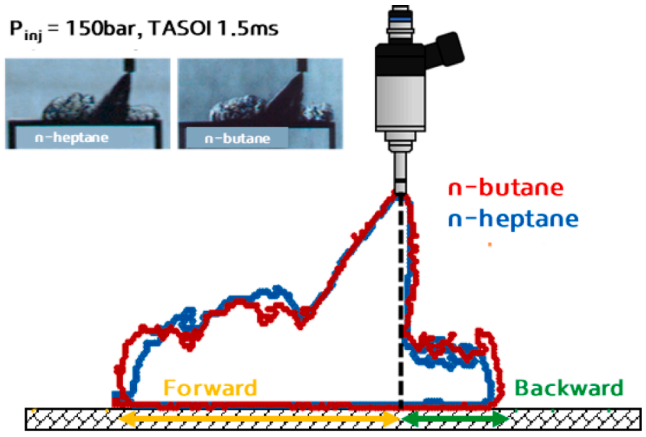

(a) Spray boundary

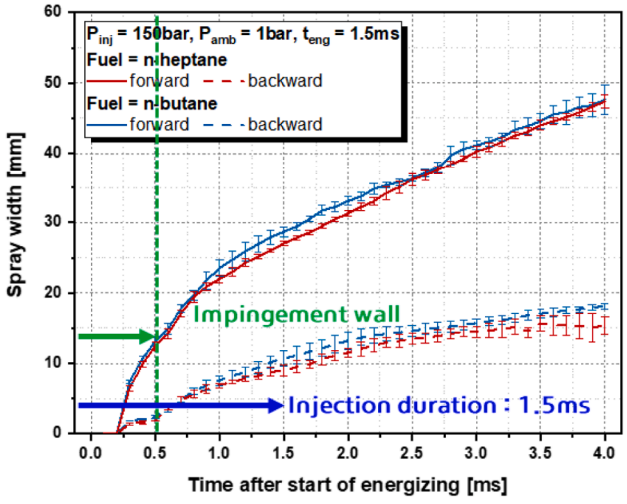

(b) Spray width

Fig. 19. Comparison of spray boundary and width.

Based on the nozzle tip wetting experiments, the average wet area of the presence of step hole injector was measured to be about 44.8 % higher than that of the absence of step hole injector at 4.00 ms. At 8.00 ms, the average wet area of two injectors increased compared to at 4.00 ms due to the surface tension of fuel property.

As a result of the PDPA experiments, no significant difference between the averaged AMD and SMD values on the spray head of two injectors was observed. However, the absence of step hole injector had slightly larger droplets than that of the presence of step hole injector, resulting in larger AMD, SMD, and droplet velocity on the spray tail.

Based on macroscopic spray characteristics as revealed by the schlieren method, the spray width and area of n-heptane exceeded those of n-butane in free spray. Unlike free spray, the spray width and area of n-butane in the flat spray were higher for n-butane compared with n-heptane.

Based on microscopic spray characteristics revealed by a PDPA, n-butane has a larger deviation of droplet diameter in flat spray compared with free spray. Unlike n-butane, n-heptane has a lower vapor pressure and higher density, and droplet diameter appears to increase flat spray due to the formation of a fuel film or rebound droplets.

Droplet velocity differs between two fuels due to fuel density at the same injection pressure and atmospheric pressure. This difference is strongly affected by the drag force of the surrounding air, which greatly affects spray atomization. The droplet speed and Weber number of n-butane were superior than those of n-heptane because of fuel properties.

CRediT authorship contribution statement

Young Soo Yu: Conceptualization, Methodology, Validation, Writing – original draft. **Yubeen Yang:** Methodology, Investigation. **Seungho Yang:** Validation, Data curation. **Dongheon Shin:** Methodology, Data curation. **Hoseung Yi:** Data curation, Investigation. **Namho Kim:** Methodology, Investigation. **Sungwook Park:** Conceptualization, Supervision, Writing – review & editing.

Declaration of Competing Interest

The authors declare that they have no known competing financial interests or personal relationships that could have appeared to influence the work reported in this paper.

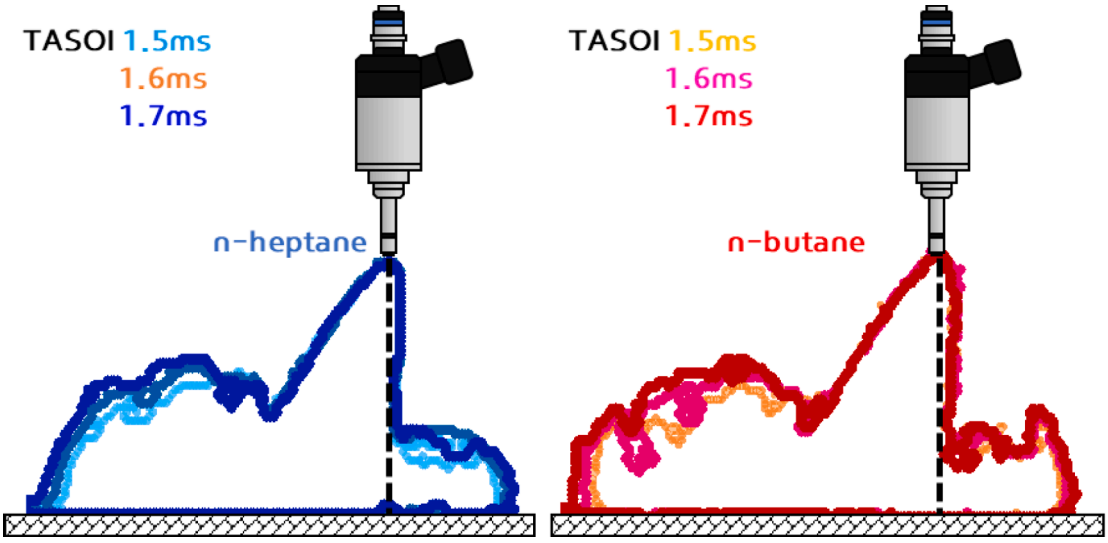

(a) Spray boundary over time

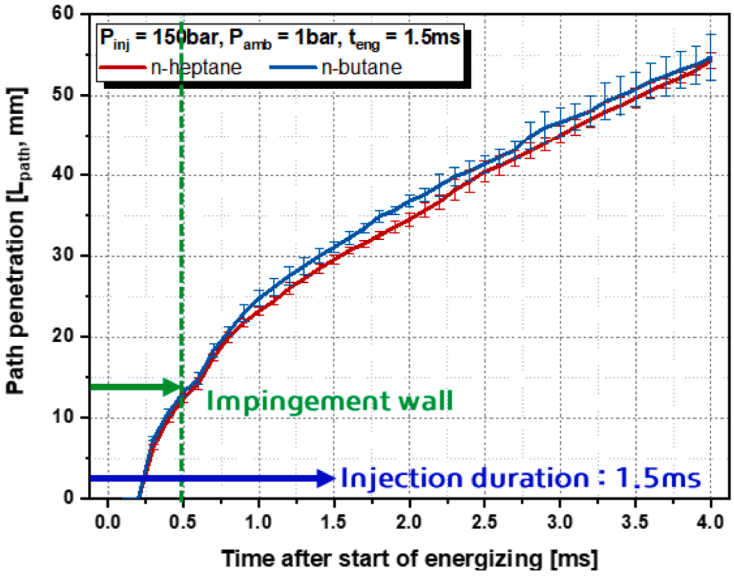

(b) Spray path penetration

Fig. 20. Spray path penetration characteristics.

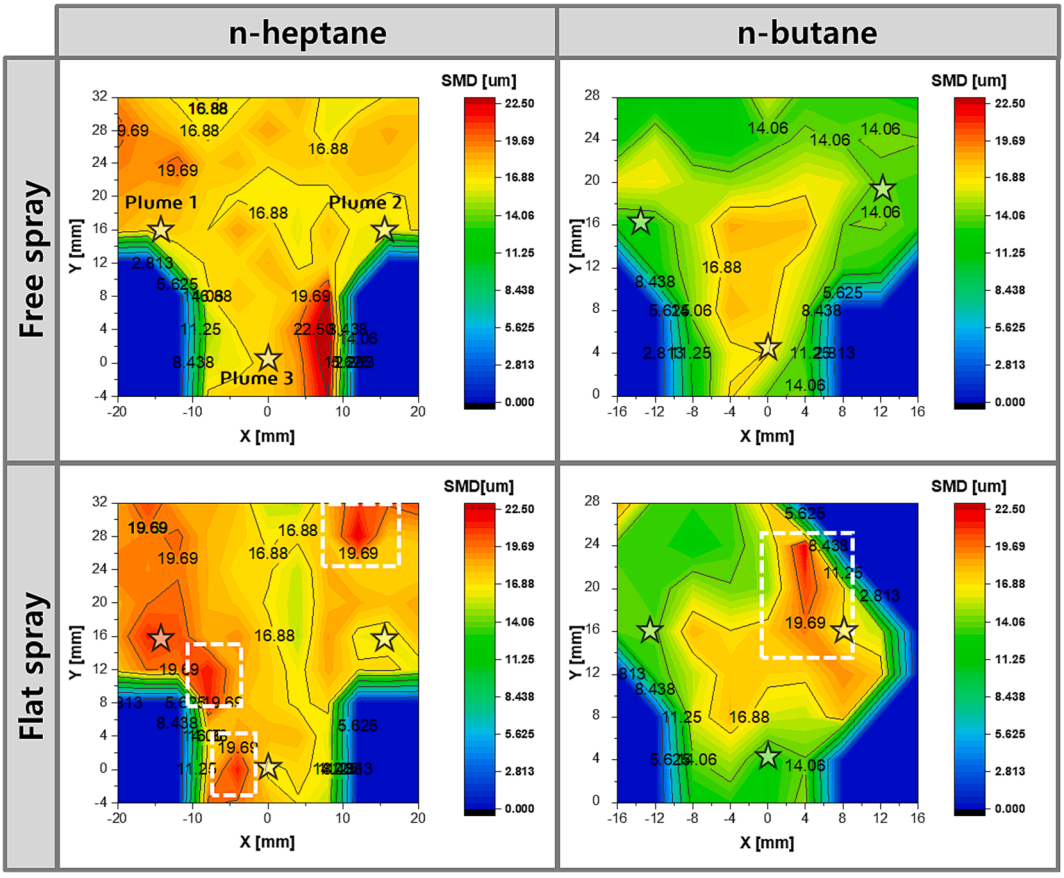

Fig. 21. Spatial dispersion of droplet diameter as function of test fuels.

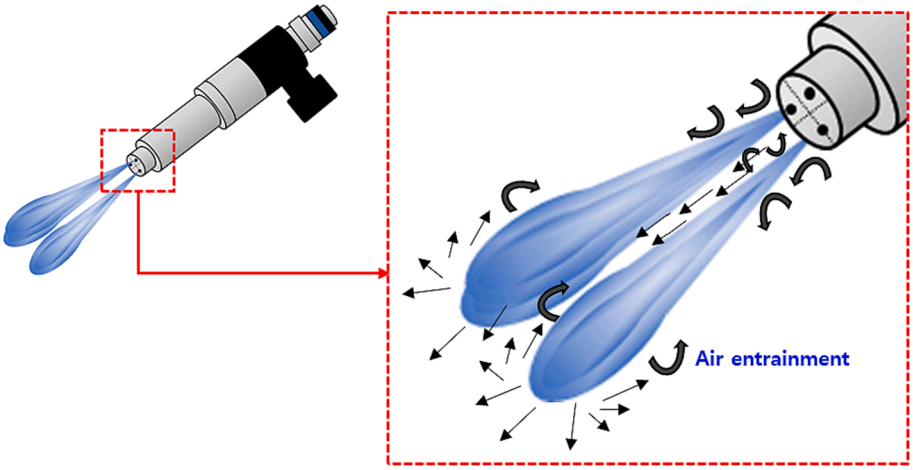

Fig. 22. Illustration of air-entrainment interaction between spray and air.

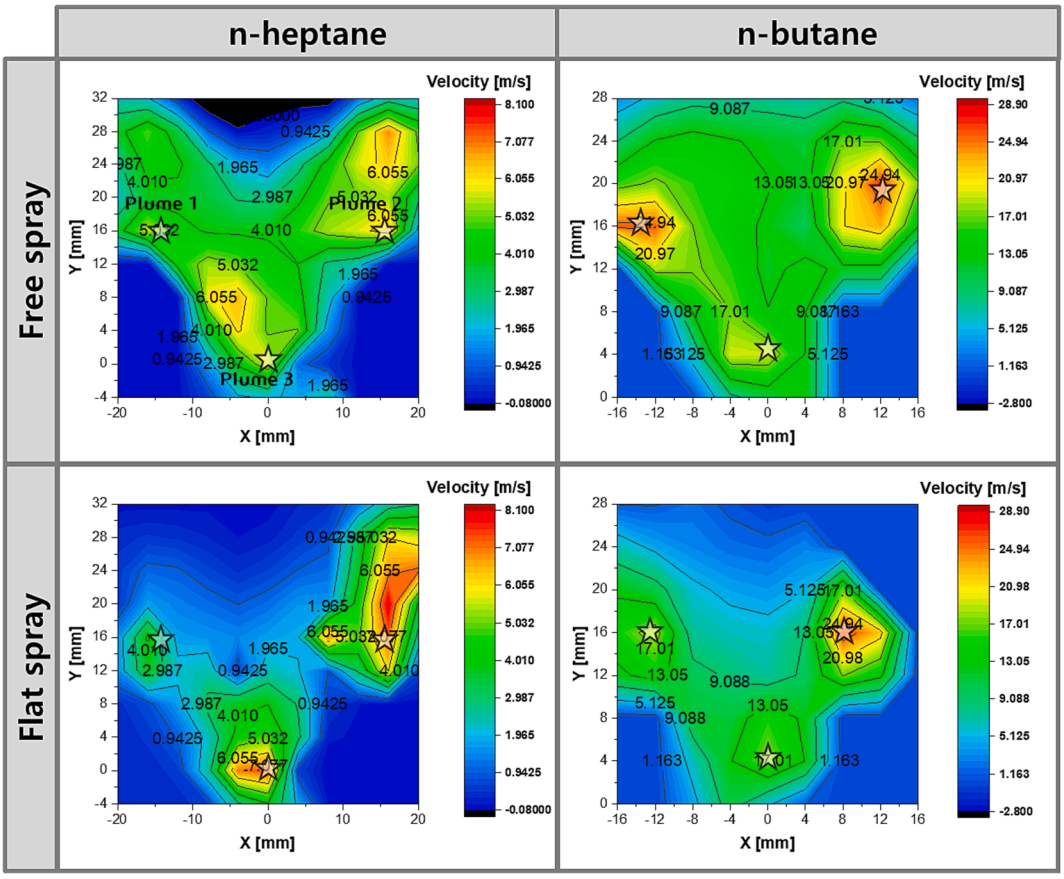

Fig. 23. Spatial dispersion of droplet velocity as function of test fuels.

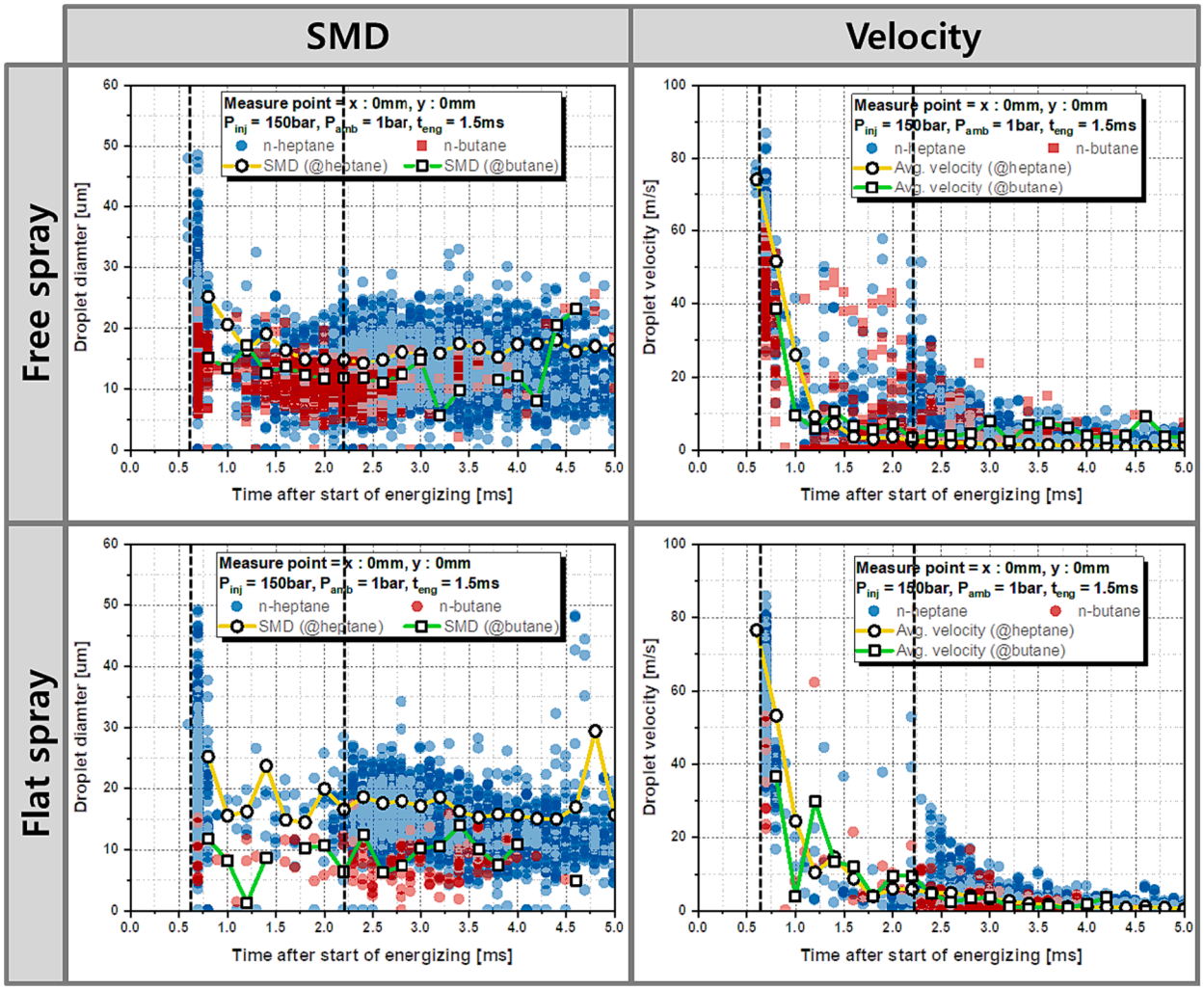

Fig. 24. Droplet diameter and velocity characteristics as function of test fuels.

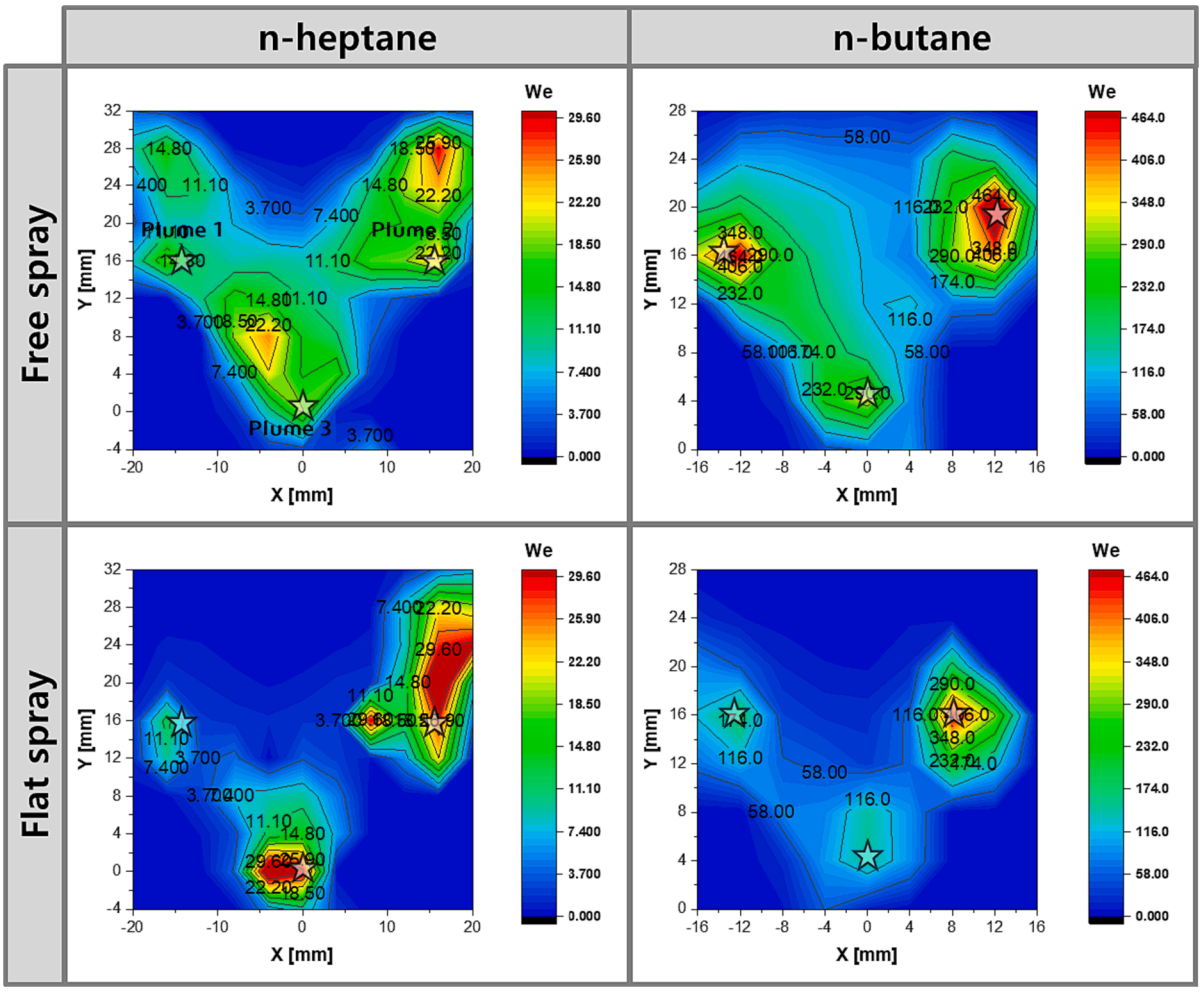

Fig. 25. Weber number characteristics as function of test fuels.

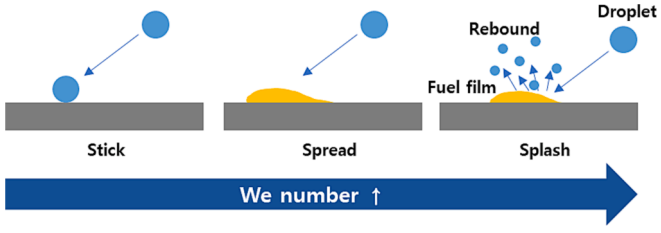

Fig. 26. Illustration of interaction between spray and wall according to weber number.

Data availability

Data will be made available on request.

Acknowledgments

This work was supported by the Korea Institute of Energy Technology Evaluation and Planning (KETEP) grant funded by the Korea government(MOTIE) (No. 20224000000440, Sector coupling energy industry advancement manpower training program).

References

[1] B. Anh, H. Dale, S. Stephanie, Advanced Clean Cars II: The next phase of California's Zero-Emission Vehicle and Low-Emission Vehicle regulations, The international council on clean transporation, 2022.
[2] EUROPEAN COMMISSION, ANNEXES to the Proposal for a Regulation of the European Parliament and the Council on type-approval of motor vehicles and engines and of systems, components and separate technical units intended for such vehicles, with respect to their emissions and battery durability (Euro 7) and repealing Regulations (EC) No 715/2007 and (EC) No 595/2009, COM(2022) 586 final, ANNEXES 1 to 6, Brussels, 2022.
[3] EUROPEAN COMMISSION-Press release, Commission proposes new Euro 7 standards to reduce pollutant emissions from vehicles and improve air quality, Brussels, 2022.
[4] Hu Z, Xu Y, Wang Z, Zhang H, Tan P, Lou D. An experimental study on particle number, micromorphology and nanostructure characteristics of particulate matter from a China VI gasoline direct injection engine. Atmospheric Environment: X 2023;18:100211.
[5] Lucking AJ, Lundback M, Barath SL, Mills NL, Sidhu MK, Langrish JP, et al. Particle traps prevent adverse vascular and prothrombotic effects of diesel engine exhaust inhalation in men. Circulation 2011;123(16):1721–8.
[6] Melaika M, Herbillon G, Dahlander P. Spark ignition engine performance, standard emissions and particulates using GDI, PFI-CNG and DI-CNG systems. Fuel 2021; 293:120454.
[7] Park C, Kim Y, Oh J, Choi J, Choi Y. Effect of fuel injection timing on performance and emissions with a dedicated direct injector in a hydrogen engine. Energy Conversion and Management: X 2023;18:100379.
[8] Lorenzo MD, Brequigny P, Foucher F, Mounaim-Rousselle C. Turbulent flame speed of a gasoline surrogate in conditions representative of modern downsized spark-ignition engine. Combustion and Flane 2022;240:112041.
[9] Shin J, Choi J, Seo J, Park S. Pre-chamber combustion system for heavy-duty engines for operating dual fuel and diesel modes. Energ Conver Manage 2022;255: 115365.

[10] Kim T, Park S. Optimizing injector nozzle hole layout of a direct-injection spark-ignition engine for wide open throttle condition. Envergy Conver Manage 2019; 181:59–67.
[11] Kim D, Son Y, Park S. Effects of operating parameters on in-cylinder flow characteristics of an optically accessible engine with a spray-guided injector. Energy 2022;245:123314.
[12] Soo Yu Y, Shin D, Jeong M, Park J, Park S. Effect on flash boiling spray characteristics in the far-field and near-field and nozzle tip wetting with multi-hole LPDI injector. Appl Therm Eng 2023;219:119676.
[13] Pham Q, Chang M, Kalwar A, Agarwal AK, Park S, Choi B, et al. Macroscopic spray characteristics and internal structure studies of natural gas injection. Energy 2023; 263:126055.
[14] Dinesh MH, Kumar GN. Effects of compression and mixing ratio on NH3/H2 fueled Si engine performance, combustion stability, and emission. Energy Conversion and Management: X 2022;15:100269.
[15] Soo Yu Y, Yang S, Jeong M, Kim H, Yi H, Hwan Park J, et al. Experimental investigations on the spray structure and nozzle tip wetting using various fuels with an LPDI injector. Fuel 2022;318:123719.
[16] Lee S, Park S. Spray atomization characteristics of a GDI injector equipped with a group-hole nozzle. Fuel 2014;137:50–9.
[17] Kim D, Park S. Spray characteristics of fouled gasoline direct injectors under flash boiling and sub-zero temperature conditions. Case Stud Ther Eng 2022;37:102259.
[18] Lee S, Park S. Experimental study on spray break-up and atomization processes from GDI injector using high injection pressure up to 30 MPa. Int J Heat Fluid Flow 2014;45:14–22.
[19] Kim H, Park S, Park S. Effects of in-nozzle flow and low-pressure zone on spray targeting of multi-hole gasoline direct injection injector. Fuel 2023;339:127356.
[20] He Z, Zhong W, Wang Q, Jiang Z, Shao Z. Effect of nozzle geometrical and dynamic factors on cavitating and turbulent flow in a diesel multi-hole injector nozzle. Int J Therm Sci 2013;70:132–43.
[21] Lee Z, Kim D, Park S. Effects of spray behavior and wall impingement on particulate matter emissions in a direct injection spark ignition engine equipped with a high pressure injection system. Energ Conver Manage 2020;213:112865.
[22] Payri R, Gilles H, Jaime G, Abian B. Analysis of counterbore effect in five diesel common rail injectors. Exp Therm Fluid Sci 2019;107:69–78.
[23] Payri R, Joaquin DLM, Javier M-S, Francesco CP, Alberto V. Impact of counter-bore nozzle on the combustion process and exhaust emissions for light-duty diesel engine application. Int J Engine Res 2019;20(1):46–57.
[24] Park J, Park S. Spray development process utilizing a multi-hole GDI injector with different spray hole lengths and step hole diameters. Int J Automot Technol 2022; 23(3):641–9.
[25] H. Oh, J. Lee, S. Han, C. Park, C. Bae, J. Lee, I.K. Seo, S.J. Kim, Effect of injector nozzle hole geometry on particulate emissions in a downsized direct injection gasoline engine, SAE technical paper 2017-24-0111, 2017.
[26] Pei Y, Qin J, Li X, Zhang D, Wang K, Liu Y. Experimental investigation on free and impingement spray fueled with methanol, ethanol, isooctane, TRF and gasoline. Fuel 2017;208:174–83.
[27] Qiu S, Xiao Di, Zhang X, Wang S, Wang T, Li X, et al. Experimental investigations of the phase change impacts on flash boiling spray propagations and impingements. Fuel 2022;312:122871.
[28] Peraza JE. ECN spray D visualization of the spray interaction with a transparent wall under engine-like condtions, Part II: impinging spray combustion. Fuel 2022; 308:121964.
[29] Surface vehicle recommended practice: Gasoline Fuel Injector Spray Measurement and Characterization, SAE International, J2715, 2007.
[30] Yang Y, Yu YS, Jeong M, Park S. Mixture formation enhancement in a direct-injection spark-ignition engine using horizontal injection. Fuel 2022;326:125121.
[31] Kook S, Le MK, Padala S, Hawkes ER. Z-type schlieren setup and its application to high-speed imaging of gasoline sprays. SAE Technical Paper 2011–01-1981, 2011..
[32] Stanton DW, Rutland CJ. Modelilng fuel film formation and wall interaction in diesel engines. SAE Trans 1996;15:808–24.
[33] Li X, Yang S, Li T, Hung DLS, Xu M. Investigations on near-field atomization of flash boiling sprays for gasoline direct injection related applications. Fuel 2019; 257:116097.
[34] Jianwei Z, Yiqiang P, Zhijun P, Yanfeng Z, Jing Q, Li W, et al. Characteristics of near-nozzle spray development from a fouled GDI injector. Fuel 2018;219:17–29.
[35] J.Y. Koo, S.T. Hong, S.S. Joseph, S. Goto, Influence of fuel injector nozzle geometry on internal and external flow characteristics, SAE Transactions, Vol. 106, Section 3: journal of engines (1997), pp. 568-580.
[36] Yan F, Du Y, Wang L, Tang W, Zhang J, Liu B, et al. Effects of injection pressure on cavitation and spray in marine diesel engine. Int J Spray Combustion Dynamics 2017;9(3):186–98.
[37] Kim B, Park S. Study on in-nozzle flow and spray behavior characteristics under various needle positions and length-to-width ratios of nozzle orifice using a transparent acrylic nozzle. Int J Heat Mass Transf 2019;143:118478.
[38] Musculus MPB, Miles PC, Pickett LM. Conceptual models for partially premixed low-temperature diesel combustion. Prog Energy Combust Sci 2013;39(2-3): 246–83.
[39] Lee SY. Liquid atomization. Korean: Mineum-sa; 1996.
[40] Guohong T, Haiying L, Hongming X, Yanfei L, Satish MR. Spray characteristics study of DMF using phase doppler particle analyzer, SAE Int. J Passeng Cars -Mech Syst 2010;3(1):948–58.
[41] Kim H, Kim J, Park S. Atomization characteristics of aerosol spray from hair spray vessel with various design parameters. J Aerosol Sci 2019;133:24–36.
[42] Tamhane TV, Joshi JB, Mudali K, Natarajan R, Patil RN. Measurement of drop size characteristics in annualr centrifugal extractors using phase doppler particle analyzer [PDPA]. Chem Eng Res Design 2012;90:985–97.
[43] Yukihiro Y, Tomoaki K. Analytical consideration of liquid droplet impingement on solid surfaces. Sci Rep 2017;7:2362.
[44] Qi W, Ming P, Peng Ye, Jilani A. Numerical investigation of the characteristics of spray/wall interaction with hybrid breakup model by considering nozzle exit turbulence. SAE Int J Engines 2019;12(1):101–13.
[45] Park J, Kim T, Kim D, Park S. Prediction of wall impingement in a direct injection spark ignition engine by analyzing spray images for high-pressure injection up to 50MPa. Fuel Process Technol 2018;179:238–49.
[46] Ma T, Feng L, Wang H, Liu H, Yao M. A numerical study of spray/wall impingement based on droplet impact phenomenon. Int J Heat Mass Transf 2017; 112:401–12.